

UC Davis

UC Davis Previously Published Works

Title

Loss of cytoplasmic incompatibility and minimal fecundity effects explain relatively low Wolbachia frequencies in *Drosophila mauritiana*

Permalink

<https://escholarship.org/uc/item/3z55k8mq>

Journal

Evolution, 73(6)

ISSN

0014-3820

Authors

Meany, Megan K
Conner, William R
Richter, Sophia V
[et al.](#)

Publication Date

2019-06-01

DOI

10.1111/evo.13745

Peer reviewed

Loss of cytoplasmic incompatibility and minimal fecundity effects explain relatively low *Wolbachia* frequencies in *Drosophila mauritiana*

Megan K. Meany¹, William R. Conner¹, Sophia V. Richter¹, Jessica A. Bailey¹, Michael Turelli² and Brandon S. Cooper^{1¶}

¹Division of Biological Sciences, University of Montana, Missoula, MT USA

²Department of Evolution and Ecology, University of California, Davis, CA USA

Correspondence:

¶Division of Biological Sciences

University of Montana

32 Campus Drive, ISB

Missoula, MT 59812, USA

Email: brandon.cooper@umontana.edu

RUNNING TITLE: *wMau Wolbachia* in *Drosophila mauritiana*

KEYWORDS

host-microbe interactions, introgression, maternal transmission, mitochondria, spatial spread, WO phage

ABSTRACT

Maternally transmitted *Wolbachia* bacteria infect about half of all insect species. Many *Wolbachia* cause cytoplasmic incompatibility (CI), reduced egg hatch when uninfected females mate with infected males. Although CI produces a frequency-dependent fitness advantage that leads to high equilibrium *Wolbachia* frequencies, it does not aid *Wolbachia* spread from low frequencies. Indeed, the fitness advantages that produce initial *Wolbachia* spread and maintain non-CI *Wolbachia* remain elusive. *wMau* *Wolbachia* infecting *Drosophila mauritiana* do not cause CI, despite being very similar to CI-causing *wNo* from *D. simulans* (0.068% sequence divergence over 682,494 bp), suggesting recent CI loss. Using draft *wMau* genomes, we identify a deletion in a CI-associated gene, consistent with theory predicting that selection within host lineages does not act to increase or maintain CI. In the laboratory, *wMau* shows near-perfect maternal transmission; but we find no significant effect on host fecundity, in contrast to published data. Intermediate *wMau* frequencies on the island Mauritius are consistent with a balance between unidentified small, positive fitness effects and imperfect maternal transmission. Our phylogenomic analyses suggest that group-B *Wolbachia*, including *wMau* and *wPip*, diverged from group-A *Wolbachia*, such as *wMel* and *wRi*, 6–46 million years ago, more recently than previously estimated.

INTRODUCTION

1 Maternally transmitted *Wolbachia* infect about half of all species throughout all major insect
2 orders (Werren and Windsor 2000; Zug and Hammerstein 2012; Weinert et al. 2015), as well as
3 other arthropods (Jeyaparakash and Hoy 2000; Hilgenboecker et al. 2008) and nematodes (Taylor
4 et al. 2013). Host species may acquire *Wolbachia* from common ancestors, from sister species
5 via hybridization and introgression, or horizontally (O'Neill et al. 1992; Rousset and Solignac
6 1995; Huigens et al. 2004; Baldo et al. 2008; Raychoudhury et al. 2009; Gerth and Bleidorn
7 2016; Schuler et al. 2016; Turelli et al. 2018). *Wolbachia* often manipulate host reproduction,
8 inducing cytoplasmic incompatibility (CI) and male killing in *Drosophila* (Laven 1951; Yen and
9 Barr 1971; Hoffmann et al. 1986; Hoffmann and Turelli 1997; Hurst and Jiggins 2000). CI
10 reduces egg hatch when *Wolbachia*-uninfected females mate with infected males. Three
11 parameters usefully approximate the frequency dynamics and equilibria of CI-causing *Wolbachia*
12 that do not distort sex ratios: the relative hatch rate of uninfected eggs fertilized by infected
13 males (H), the fitness of infected females relative to uninfected females (F), and the proportion
14 of uninfected ova produced by infected females (μ) (Caspari and Watson 1959; Hoffmann et al.
15 1990). To spread deterministically from low frequencies, *Wolbachia* must produce $F(1 - \mu) > 1$,
16 irrespective of CI. Once they become sufficiently common, CI-causing infections, such as *w*Ri-
17 like *Wolbachia* in *Drosophila simulans* and several other *Drosophila* (Turelli et al. 2018), spread
18 to high equilibrium frequencies, dominated by a balance between CI and imperfect maternal
19 transmission (Turelli and Hoffmann 1995; Kreisner et al. 2016). In contrast, non-CI-causing
20 *Wolbachia*, such as *w*Au in *D. simulans* (Hoffmann et al. 1996), typically persist at lower
21 frequencies, presumably maintained by a balance between positive *Wolbachia* effects on host
22 fitness and imperfect maternal transmission (Hoffmann and Turelli 1997; Kreisner et al. 2013).
23 When $H < F(1 - \mu) < 1$, “bistable” dynamics result, producing stable equilibria at 0 and at a
24 higher frequency denoted p_s , where $0.50 < p_s \leq 1$ (Turelli and Hoffmann 1995). Bistability
25 explains the pattern and (slow) rate of spread of *w*Mel transinfected into *Aedes aegypti* to
26 suppress the spread of dengue, Zika and other human diseases (Hoffmann et al. 2011; Barton and
27 Turelli 2011; Turelli and Barton 2017; Schmidt et al. 2017).

28 In contrast to the bistability observed with *w*Mel transinfections, natural *Wolbachia*
29 infections seem to spread via “Fisherian” dynamics with $F(1 - \mu) > 1$ (Fisher 1937; Kreisner et
30 al. 2013; Hamm et al. 2014). Several *Wolbachia* effects could generate $F(1 - \mu) > 1$, but we do

31 not yet know which ones actually do. For example, *w*Ri has evolved to increase *D. simulans*
32 fecundity in only a few decades (Weeks et al. 2007), *w*Mel seems to enhance *D. melanogaster*
33 fitness in high and low iron environments (Brownlie et al. 2009), and several *Wolbachia*
34 including *w*Mel protect their *Drosophila* hosts from RNA viruses (Hedges et al. 2008; Teixeira
35 et al. 2008; Martinez et al. 2014). However, it remains unknown which if any these potential
36 fitness benefits underlie *Wolbachia* spread in nature. For instance, *w*Mel seems to have little
37 effect on viral abundance in wild-caught *D. melanogaster* (Webster et al. 2015; Shi et al. 2018).

38 *D. mauritiana*, *D. simulans* and *D. sechellia* comprise the *D. simulans* clade within the nine-
39 species *D. melanogaster* subgroup of *Drosophila*. The *D. simulans* clade diverged from *D.*
40 *melanogaster* approximately three million years ago (mya), with the island endemics *D. sechellia*
41 (Seychelles archipelago) and *D. mauritiana* (Mauritius) thought to originate in only the last few
42 hundred thousand years (Lachaise et al. 1986; Ballard 2000a; Dean and Ballard 2004;
43 McDermott and Kliman 2008; Garrigan et al. 2012; Brand et al. 2013; Garrigan et al. 2014). *D.*
44 *simulans* is widely distributed around the globe, but has never been collected on Mauritius
45 (David et al. 1989; Legrand et al. 2011). However, evidence of mitochondrial and nuclear
46 introgression supports interisland migration and hybridization between these species (Ballard
47 2000a; Nunes et al. 2010; Garrigan et al. 2012), which could allow introgressive *Wolbachia*
48 transfer (Rousset and Solignac 1995).

49 *D. mauritiana* is infected with *Wolbachia* denoted *w*Mau, likely acquired via introgression
50 from other *D. simulans*-clade hosts (Rousset and Solignac 1995). *Wolbachia* variant *w*Mau may
51 also infect *D. simulans* (denoted *w*Ma in *D. simulans*) in Madagascar and elsewhere in Africa
52 and the South Pacific (Ballard 2000a; Ballard 2004). *w*Mau does not cause CI in *D. mauritiana*
53 or when transinfected into *D. simulans* (Giordano et al. 1995). Yet it is very closely related to
54 *w*No strains that do cause CI in *D. simulans* (Merçot et al. 1995; Rousset and Solignac 1995;
55 James and Ballard 2000, 2002). (Also, *D. simulans* seems to be a “permissive” host for CI, as
56 evidenced by the fact that *w*Mel, which causes little CI in its native host, *D. melanogaster*,
57 causes intense CI in *D. simulans* [Poinsot et al. 1998].) Fast et al. (2011) reported that a *w*Mau
58 variant increased *D. mauritiana* fecundity four-fold. This fecundity effect occurred in concert
59 with *w*Mau-induced alternations of programmed cell death in the germarium and of germline
60 stem cell mitosis, possibly providing insight into the mechanisms underlying increased egg

61 production (Fast et al. 2011). However, the generality of this finding across *w*Mau variants and
62 host genetic backgrounds remains unknown.

63 Here, we assess the genetic and phenotypic basis of *w*Mau frequencies in *D. mauritiana* on
64 Mauritius by combining analysis of *w*Mau draft genomes with analysis of *w*Mau transmission in
65 the laboratory and *w*Mau effects on host fecundity and egg hatch. We identify a single mutation
66 that disrupts a locus associated with CI. The loss of CI in *w*Mau is consistent with theory
67 demonstrating that selection within host species does not act to increase or maintain the level of
68 CI (Prout 1994; Turelli 1994; Haygood and Turelli 2009), but instead acts to increase $F(1 - \mu)$,
69 the product of *Wolbachia* effects on host fitness and maternal transmission efficiency (Turelli
70 1994). The loss of CI helps explain the intermediate *w*Mau frequencies on Mauritius, reported by
71 us and Giordano et al. (1995). We find no *w*Mau effects on host fecundity, and theoretical
72 analyses show that even a two-fold fecundity increase cannot be reconciled with the observed
73 intermediate population frequencies, unless maternal *w*Mau transmission is exceptionally
74 unreliable in the field. Finally, we present theoretical analyses illustrating that the persistence of
75 two distinct classes of mtDNA haplotypes among *Wolbachia*-uninfected *D. mauritiana* is
76 unexpected under a simple null model. Together, our results contribute to understanding the
77 genomic and phenotypic basis of global *Wolbachia* persistence, which is relevant to improving
78 *Wolbachia*-based biocontrol of human diseases (Ritchie 2018).

79

80 MATERIALS AND METHODS

81 *Drosophila* Husbandry and Stocks

82 The *D. mauritiana* isofemale lines used in this study ($N = 32$) were sampled from Mauritius in
83 2006 by Margarita Womack and kindly provided to us by Prof. Daniel Matute from the
84 University of North Carolina, Chapel Hill. We also obtained four *D. simulans* stocks (lines 196,
85 297, 298, and 299) from the National *Drosophila* Species Stock Center that were sampled from
86 Madagascar. Stocks were maintained on modified version of the standard Bloomington-cornmeal
87 medium (Bloomington Stock Center, Bloomington, IN) and were kept at 25°C, 12 light:12 dark
88 photoperiod prior to the start of our experiments.

89

90

91

92 **Determining *Wolbachia* infection status and comparing infection frequencies**

93 One to two generations prior to our experiments DNA was extracted from each isofemale line
94 using a standard ‘squish’ buffer protocol (Gloor et al. 1993), and infection status was determined
95 using a polymerase chain reaction (PCR) assay (Simpliamp ThermoCycler, Applied Biosystems,
96 Singapore). We amplified the *Wolbachia*-specific *wsp* gene (Forward: 5’-
97 TGGTCCAATAAGTGATGAAGAAAC-3’; Reverse: 5’-AAAAATTAAACGCTACTCCA-3’;
98 Braig et al. 1998) and a nuclear control region of the *2L* chromosome (Forward: 5’-
99 TGCAGCTATGGTCGTTGACA-3’; Reverse: 5’-ACGAGACAATAATATGTGGTGCTG-3’;
100 designed here). PCR products were visualized using 1% agarose gels that included a molecular-
101 weight ladder. Assuming a binomial distribution, we estimated exact 95% binomial confidence
102 intervals for the infection frequencies on Mauritius. Using Fisher’s Exact Test, we tested for
103 temporal differences in *w*Mau frequencies by comparing our frequency estimate to a previous
104 estimate (Giordano et al. 1995). All analyses were performed using R version 3.5.1 (R Team
105 2015).

106 We used quantitative PCR (qPCR) (MX3000P, Agilent Technologies, Germany) to confirm
107 that tetracycline-treated flies were cleared of *w*Mau. DNA was extracted from *D. mauritiana*
108 flies after four generations of tetracycline treatment (1-2 generations prior to completing our
109 experiments), as described below. Our qPCR used a PowerUp™ SYBR™ Green Master Mix
110 (Applied Biosystems™, California, USA) and amplified *Wolbachia*-specific *wsp* (Forward: 5’-
111 CATTGGTGTTGGTGGTGGTG-3’; Reverse: 5’-ACCGAAATAACGAGCTCCAG-3’) and
112 *Rpl32* as a nuclear control (Forward: 5’-CCGCTTCAAGGGACAGTATC-3’; Reverse: 5’-
113 CAATCTCCTTGCGCTTCTTG-3’;
114 Newton and Sheehan 2014).

115

116 ***Wolbachia* DNA extraction, library preparation, and sequencing**

117 We sequenced *w*Mau-infected *R9*, *R29*, and *R60* *D. mauritiana* genotypes. Tissue samples for
118 genomic DNA were extracted using a modified CTAB Genomic DNA Extraction protocol. DNA
119 quantity was tested on an Implen Nanodrop (Implen, München, Germany) and total DNA was
120 quantified by Qubit Fluorometric Quantitation (Invitrogen, Carlsbad, California, USA). DNA
121 was cleaned using Agencourt AMPure XP beads (Beckman Coulter, Inc., Brea, CA, U.S.A),
122 following manufacturers’ instructions, and eluted in 50 µl 1× TE Buffer for shearing. DNA was

123 sheared using a Covaris E220 Focused Ultrasonicator (Covaris Inc., Woburn, MA) to a target
124 size of 400 bp. We prepared libraries using NEBNext® Ultra™ II DNA Library Prep with
125 Sample Purification Beads (New England BioLabs, Ipswich, Massachusetts). Final fragment
126 sizes and concentrations were confirmed using a TapeStation 2200 system (Agilent, Santa Clara,
127 California). We indexed samples using NEBNext® Multiplex Oligos for Illumina® (Index
128 Primers Set 3 & Index Primers Set 4), and 10 µl of each sample was shipped to Novogene
129 (Sacramento, CA) for sequencing using Illumina HiSeq 4000 (San Diego, CA), generating
130 paired-end, 150 bp reads.

131

132 ***Wolbachia* assembly**

133 We obtained published reads ($N = 6$) from Garrigan et al. (2014), and assembled these genomes
134 along with the *R9*, *R29*, and *R60* genomes that we sequenced. Reads were trimmed using Sickle
135 v. 1.33 (Joshi and Fass 2011) and assembled using ABySS v. 2.0.2 (Jackman et al. 2017). *K*
136 values of 41, 51, 61, and 71 were used, and scaffolds with the best nucleotide BLAST matches to
137 known *Wolbachia* sequences with E-values less than 10^{-10} were extracted as the draft *Wolbachia*
138 assemblies. We deemed samples infected if the largest *Wolbachia* assembly was at least 1
139 million bases and uninfected if the largest assembly was fewer than 100,000 bases. No samples
140 produced *Wolbachia* assemblies between 100,000 and 1 million bases. Of the six sets of
141 published reads we analyzed (Garrigan et al. 2014), only lines *R31* and *R41* were *wMau*-infected.
142 We also screened the living copies of these lines for *wsp* using PCR, and both were infected,
143 supporting reliable *wMau* transmission in the lab since these lines were sampled in nature.

144 To assess the quality of our draft assemblies, we used BUSCO v. 3.0.0 to search for
145 homologs of the near-universal, single-copy genes in the BUSCO proteobacteria database
146 (Simao et al. 2015). As a control, we performed the same search using the reference genomes for
147 *wRi* (Klasson et al. 2009), *wAu* (Sutton et al. 2014), *wMel* (Wu et al. 2004), *wHa* (Ellegaard et
148 al. 2013), and *wNo* (Ellegaard et al. 2013).

149

150 ***Wolbachia* gene extraction and phylogenetics**

151 To determine phylogenetic relationships and estimate divergence times, we obtained the public
152 *Wolbachia* group-B genomes of: *wAlbB* that infects *Aedes albopictus* (Mavingui et al. 2012),
153 *wPip_Pel* that infects *Culex pipiens* (Klasson et al. 2008), *wPip_Mol* that infects *Culex molestus*

154 (Pinto et al. 2013), *wNo* that infects *Drosophila simulans* (Ellegaard et al. 2013), and *wVitB* that
155 infects *Nasonia vitripennis* (Kent et al. 2011); in addition to group-A genomes of: *wMel* that
156 infects *D. melanogaster* (Wu et al. 2004), *wSuz* that infects *D. sukuzii* (Siozios et al. 2013), four
157 *Wolbachia* that infect *Nomada* bees (*wNFe*, *wNPa*, *wNLeu*, and *wNFa*; Gerth and Bleidorn
158 2016), and three *Wolbachia* that infect *D. simulans* (*wRi*, *wAu* and *wHa*; Klasson et al. 2009;
159 Sutton et al. 2014; Ellegaard et al. 2013). The previously published genomes and the five *wMau*-
160 infected *D. mauritiana* genomes were annotated with Prokka v. 1.11, which identifies homologs
161 to known bacterial genes (Seemann 2014). To avoid pseudogenes and paralogs, we used only
162 genes present in a single copy, and with no alignment gaps, in all of the genome sequences.
163 Genes were identified as single copy if they uniquely matched a bacterial reference gene
164 identified by Prokka v. 1.11. By requiring all homologs to have identical length in all of the draft
165 *Wolbachia* genomes, we removed all loci with indels. 143 genes, a total of 113,943 bp, met these
166 criteria when comparing all of these genomes. However, when our analysis was restricted to the
167 five *wMau* genomes, our criteria were met by 694 genes, totaling 704,613 bp. Including *wNo*
168 with the five *wMau* genomes reduced our set to 671 genes with 682,494 bp. We calculated the
169 percent differences for the three codon positions within *wMau* and between *wMau* and *wNo*.

170 We estimated a Bayesian phylogram of the *Wolbachia* sequences with RevBayes 1.0.8
171 under the GTR + Γ model, partitioning by codon position (Höhna et al. 2016). Four independent
172 runs were performed, which all agreed.

173 We estimated a chronogram from the *Wolbachia* sequences using the absolute chronogram
174 procedure implemented in Turelli et al. (2018). Briefly, we generated a relative relaxed-clock
175 chronogram with the GTR + Γ model with the root age fixed to 1 and the data partitioned by
176 codon position. The relaxed clock branch rate prior was $\Gamma(2,2)$. We used substitution-rate
177 estimates of $\Gamma(7,7) \times 6.87 \times 10^{-9}$ substitutions/3rd position site/year to transform the relative
178 chronogram into an absolute chronogram. This rate estimate was chosen so that the upper and
179 lower credible intervals matched the posterior distribution estimated by Richardson et al. (2012),
180 assuming 10 generations/year, normalized by their median estimate of 6.87×10^{-9} substitutions/3rd
181 position site/year. Although our relaxed-clock analyses allow for variation in substitution rates
182 across branches, our conversion to absolute time depends on the unverified assumption that the
183 median substitution rate estimated by Richardson et al. (2012) for *wMel* is relevant across these
184 broadly diverged *Wolbachia*. (To assess the robustness of our conclusions to model assumptions,

185 we also performed a strict-clock analysis and a relaxed-clock analysis with branch-rate prior
186 $\Gamma(7,7)$.) For each analysis, four independent runs were performed, which all agreed. Our analyses
187 all support *wNo* as sister to *wMau*.

188 We also estimated a relative chronogram for the host species using the procedure
189 implemented in Turelli et al. (2018). Our host phylogeny was based on the same 20 nuclear
190 genes used in Turelli et al. (2018): *aconitase*, *aldolase*, *bicoid*, *ebony*, *enolase*, *esc*, *g6pdh*, *glyp*,
191 *glys*, *ninaE*, *pepck*, *pgi*, *pgm*, *pic*, *ptc*, *tpi*, *transaldolase*, *white*, *wingless* and *yellow*.

192

193 **Analysis of *Wolbachia* and mitochondrial genomes**

194 We looked for copy number variation (CNV) between *wMau* and its closest relative, *wNo* across
195 the whole *wNo* genome. Reads from the five infected *wMau* lines were aligned to the *wNo*
196 reference (Ellegaard et al. 2013) with bwa 0.7.12 (Li and Durbin 2009). We calculated the
197 normalized read depth for each alignment over sliding 1,000-bp windows by dividing the
198 average depth in the window by the average depth over the entire *wNo* genome. The results were
199 plotted and visually inspected for putative copy number variants (CNVs). The locations of CNVs
200 were specifically identified with ControlFREEC v. 11.5 (Boeva et al. 2012), using a ploidy of
201 one and a window size of 1,000. We calculated *P*-values for each identified CNV with the
202 Wilcoxon Rank Sum and the Kolmogorov-Smirnov tests implemented in ControlFREEC.

203 We used BLAST to search for pairs of CI-factor (*cif*) homologs in *wMau* and *wNo* genomes
204 that are associated with CI (Beckmann and Fallon 2013; Beckmann et al. 2017; LePage et al.
205 2017; Lindsey et al. 2018; Beckmann et al. 2018). (We adopt Beckmann et al. (2019)'s
206 nomenclature that assigns names to loci based on their predicted enzymatic function, with
207 superscripts denoting the focal *Wolbachia* strain.) These include predicted CI-inducing
208 deubiquitylase (*cid*) *wPip_0282-wPip_0283* (*cidA-cidB^{wPip}*) and CI-inducing nuclease (*cin*)
209 *wPip_0294-wPip_0295* (*cinA-cinB^{wPip}*) pairs that induce toxicity and rescue when expressed/co-
210 expressed in *Saccharomyces cerevisiae* (Beckmann et al. 2017 and Beckmann et al. 2018);
211 WD0631-WD632 (*cidA-cidB^{wMel}*) that recapitulate CI when transgenically expressed in *D.*
212 *melanogaster* (LePage et al. 2017); and *wNo_RS01055* and *wNo_RS01050* that have been
213 identified as a Type III *cifA-cifB* pair in the *wNo* genome (LePage et al. 2017; Lindsey et al.
214 2018). *wNo_RS01055* and *wNo_RS01050* are highly diverged from *cidA-cidB^{wMel}* and *cidA-*
215 *cidB^{wPip}* homologs and from *cinA-cinB^{wPip}*; however, this *wNo* pair is more similar to *cinA-*

216 *cinB*^{wPip} in terms of protein domains, lacking a ubiquitin-like protease domain (Lindsey et al.
217 2018). We refer to these loci as *cinA-cinB*^{wNo}.

218 We found only homologs of the *cinA-cinB*^{wNo} pair in *wMau* genomes, which we extracted
219 from our draft *wMau* assemblies and aligned with MAFFT v. 7 (Kato and Standley 2013). We
220 compared *cinA-cinB*^{wNo} to the *wMau* homologs to identify single nucleotide variants (SNVs)
221 among our *wMau* assemblies.

222 *D. mauritiana* carry either the *maI* mitochondrial haplotype, associated with *wMau*
223 infections, or the *maII* haplotype (Rousset and Solignac 1995; Ballard 2000a; James and Ballard
224 2000). To determine the mitochondrial haplotype of each *D. mauritiana* line, we assembled the
225 mitochondrial genomes by down-sampling the reads by a factor of 100, then assembling with
226 ABySS 2.0.2 using a *K* value of 71 for our data (150 bp reads) and 35 for the published data (76
227 bp reads) (Garrigan et al. 2014). Down-sampling reads prevents the nuclear genome from
228 assembling but does not inhibit assembly of the mitochondrial genome, which has much higher
229 coverage. We deemed the mitochondrial assembly complete if all 13 protein-coding genes were
230 present on the same contig and in the same order as in *D. melanogaster*. If the first attempt did
231 not produce a complete mitochondrial assembly, we adjusted the down-sampling fraction until a
232 complete assembly was produced for each line.

233 Annotated reference mitochondrial sequences for the *D. mauritiana* mitochondrial
234 haplotypes *maI* and *maII* were obtained from Ballard et al. (2000b), and the 13 protein-coding
235 genes were extracted from our assemblies using BLAST and aligned to these references. The
236 *maI* and *maII* reference sequences differ at 343 nucleotides over these protein-coding regions.
237 We identified our lines as carrying the *maI* haplotype if they differed by fewer than five
238 nucleotides from the *maI* reference and as *maII* if they differed by fewer than five nucleotides
239 from the *maII* reference. None of our assemblies differed from both references at five or more
240 nucleotides.

241

242 ***wMau* phenotypic analyses**

243 Previous analyses have demonstrated that *wMau* does not cause CI (Giordano et al. 1995). To
244 check the generality of this result, we reciprocally crossed *wMau*-infected *R3I D. mauritiana*
245 with uninfected *R4* and measured egg hatch. Flies were reared under controlled conditions at
246 25°C for multiple generations leading up to the experiment. We paired 1–2-day-old virgin

247 females with 1–2-day-old males in a vial containing spoons with cornmeal media and yeast
248 paste. After 24 hr, pairs were transferred to new spoons, and this process was repeated for five
249 days. Eggs on each spoon were given 24 hr at 25°C to hatch after flies were removed. To test for
250 CI, we used nonparametric Wilcoxon tests to compare egg hatch between reciprocal crosses that
251 produced at least 10 eggs. All experiments were carried out at 25°C with a 12 light:12 dark
252 photoperiod.

253 To determine if *wMau* generally enhances *D. mauritiana* fecundity, we assessed the
254 fecundity of two *wMau*-infected isofemale lines from Mauritius (*R31* and *R41*); we also
255 reciprocally introgressed *wMau* from each of these lines to assess host effects. To do this we
256 crossed *R31* females with *R41* males and backcrossed F₁ females to *R41* males—this was
257 repeated for four generations to generate the reciprocally introgressed *R41*^{*R31*} genotypes (*wMau*
258 variant denoted by superscripts). A similar approach was taken to generate *R31*^{*R41*} genotypes.
259 This approach has previously revealed *D. teissieri*-host effects on *wTei*-induced CI (Cooper et al.
260 2017). To assay fecundity, we reciprocally crossed each genotype (*R31*, *R41*, *R31*^{*R41*}, *R31*^{*R41*}) to
261 uninfected line *R4* to generate paired infected- and uninfected-F₁ females with similar genetic
262 backgrounds. The *wMau*-infected and uninfected F₁ females were collected as virgins and placed
263 in holding vials. We paired 3–7-day-old females individually with an uninfected-*R4* male (to
264 stimulate oviposition) in vials containing a small spoon filled with standard cornmeal medium
265 and coated with a thin layer of yeast paste. We allowed females to lay eggs for 24 hours, after
266 which pairs were transferred to new vials. This was repeated for five days. At the end of each 24-
267 hr period, spoons were frozen until counted. All experiments were carried out at 25°C with a 12
268 light:12 dark photoperiod.

269 We also measured egg lay of *wMau*-infected (*R31*) and tetracycline-cleared uninfected
270 (*R31-tet*) genotypes over 24 days, on apple-agar plates, to more closely mimic the methods of
271 Fast et al. (2011). We fed flies 0.03% tetracycline concentrated medium for four generations to
272 generate the *R31-tet* genotype. We screened F₁ and F₂ individuals for *wMau* using PCR, and we
273 then fed flies tetracycline food for two additional generations. In the fourth generation, we
274 assessed *wMau* titer using qPCR to confirm that each genotype was cleared of *wMau* infection.
275 We reconstituted the gut microbiome by rearing *R31-tet* flies on food where *R31* males had fed
276 and defecated for 48 hours. Flies were given at least three more generations to avoid detrimental
277 effects of tetracycline treatment on mitochondrial function (Ballard and Melvin 2007). We then

278 paired individual 6–7-day-old virgin *R31* ($N = 30$) and *R31-tet* ($N = 30$) females in bottles on
279 yeasted apple-juice agar plates with an *R4* male to stimulate oviposition. Pairs were placed on
280 new egg-lay plates every 24 hrs. After two weeks, we added one or two additional *R4* males to
281 each bottle to replace any dead males and to ensure that females were not sperm limited as they
282 aged.

283 We used nonparametric Wilcoxon tests to assess *wMau* effects on host fecundity. We then
284 estimated the fitness parameter F in the standard discrete-generation model of CI (Hoffmann et
285 al. 1990; Turelli 1994). We used the ‘*pwr.t2n.test*’ function in the ‘*pwr*’ library in R to assess the
286 power of our data to detect increases to F . Pairs that laid fewer than 10 eggs across each
287 experiment were excluded from analyses, but our results are robust to this threshold.

288 To estimate the fidelity of maternal transmission, *R31* and *R41* females were reared at 25°C
289 for several generations prior to our experiment. In the experimental generation, 3-5 day old
290 inseminated females were placed individually in vials that also contained two males. These *R31*
291 ($N = 17$) and *R41* ($N = 19$) sublines were allowed to lay eggs for one week. In the following
292 generation we screened F1 offspring for *wMau* infection using PCR as described above.

293

294 **RESULTS**

295 ***Wolbachia* infection status**

296 Out of 32 *D. mauritiana* lines that we analyzed, 11 were infected with *wMau Wolbachia*
297 (infection frequency = 0.34; binomial confidence interval: 0.19, 0.53). In contrast, none of the *D.*
298 *simulans* stocks ($N = 4$) sampled from Madagascar were infected, precluding our ability to
299 directly compare *wMau* and *wMa*. Our new *wMau* frequency estimate is not statistically different
300 from a previous estimate (Giordano et al. 1995: infection frequency, 0.46; binomial confidence
301 interval, (0.34, 0.58); Fisher’s Exact Test, $P = 0.293$), based largely on assaying a heterogenous
302 collection of stocks in various laboratories. These relatively low infection frequencies are
303 consistent with theoretical expectations given that *wMau* does not cause CI (Giordano et al.
304 1995; our data reported below). The intermediate *wMau* frequencies on Mauritius suggest that
305 *wMau* persists at a balance between positive effects on host fitness and imperfect maternal
306 transmission. Quantitative predictions, based on the idealized model of Hoffmann and Turelli
307 (1997), are discussed below. The maintenance of *wMau* is potentially analogous to the
308 persistence of other non-CI-causing *Wolbachia*, specifically *wAu* in some Australian populations

309 of *D. simulans* (Hoffmann et al. 1996; Kriesner et al. 2013) and *wSuz* in *D. suzukii* and *wSpc* in
310 *D. subpulchrella* (Hamm et al. 2014; Conner et al. 2017; Turelli et al. 2018; but see Cattell et al.
311 2018).

312

313 **Draft *wMau* genome assemblies and comparison to *wNo***

314 The five *wMau* draft genomes we assembled were of very similar quality (Supplemental Table
315 1). N50 values ranged from 60,027 to 63,676 base pairs, and our assemblies varied in total length
316 from 1,266,004 bases to 1,303,156 bases (Supplemental Table 1). Our BUSCO search found
317 exactly the same genes in each draft assembly, and the presence/absence of genes in our *wMau*
318 assemblies was comparable to those in the complete genomes used as controls (Supplemental
319 Table 2). In comparing our five *wMau* draft genomes over 694 single-copy, equal-length loci
320 comprising 704,613 bp, we found only one SNP. Four sequences (*R9*, *R31*, *R41* and *R60*) are
321 identical at all 704,613 bp. *R29* differs from them at a single nucleotide, a nonsynonymous
322 substitution in a locus which Prokka v. 1.11 annotates as “bifunctional DNA-directed RNA
323 polymerase subunit beta/beta.”

324 Comparing these five *wMau* sequences to the *wNo* reference (Ellegaard et al. 2013) over
325 671 genes with 682,494 bp, they differ by 0.068% overall, with equivalent divergence at all three
326 codon positions (0.067%, 0.061%, and 0.076%, respectively).

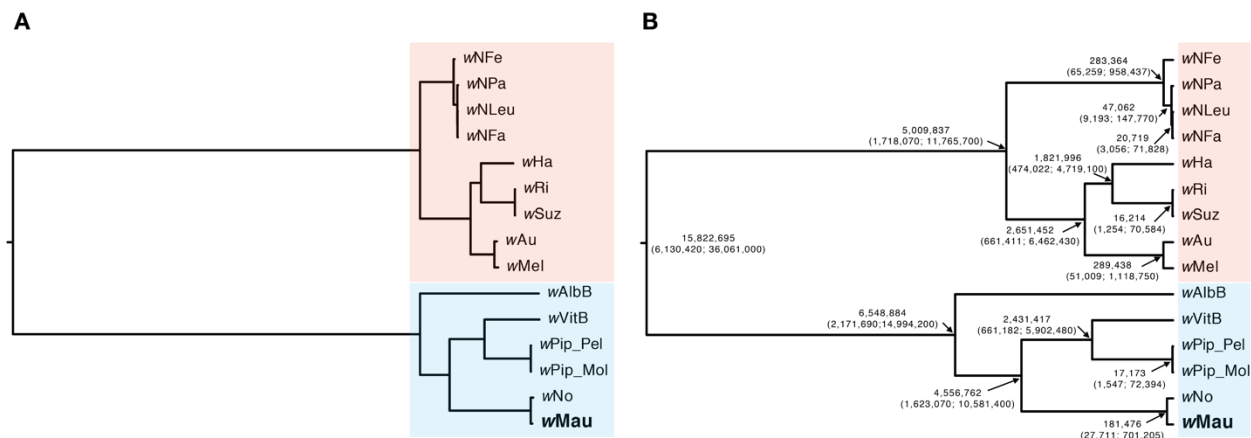
327

328 ***Wolbachia* phylogenetics**

329 As expected from the sequence comparisons, our group-B phylogram places *wMau* sister to *wNo*
330 (Figure 1A). This is consistent with previous analyses using fewer loci that placed *wMau* (or
331 *wMa* in *D. simulans*) sister to *wNo* (James and Ballard 2000; Zabalou et al. 2008; Toomey et al.
332 2013). Our chronogram (Figure 1B) estimates the 95% credible interval for the split between the
333 group-B versus group-A *Wolbachia* strains as 6 to 36 mya (point estimate, 16 mya). Reducing
334 the variance on the substitution-rate-variation prior by using $\Gamma(7,7)$ rather than $\Gamma(2,2)$, changes
335 the credible interval for the A-B split to 8 to 46 mya (point estimate, 21 mya). In contrast, a strict
336 clock analysis produces a credible interval of 12 to 64 mya (point estimate, 31 mya). These
337 estimates are roughly comparable to an earlier result based on a general approximation for the
338 synonymous substitution rate in bacteria (Ochman and Wilson 1987) and data from only the *ftsZ*
339 locus (59–67 mya, Werren et al. 1995). However, our estimates are much lower than an

340 alternative estimate based on comparative genomics (217 mya, Gerth and Bleidorn 2016). We
 341 discuss this discrepancy below.

342 The observed divergence between *wNo* and *wMau* is consistent across all three codon
 343 positions, similar to other recent *Wolbachia* splits like that between *wRi* and *wSuz* (Turelli et al.
 344 2018). Conversely, observed divergence at each codon position generally varies across the
 345 chronogram, leading to inflation of the *wNo-wMau* (181,476 years; credible interval = 27,711 to
 346 701,205 years; Figure 1B) and *wRi-wSuz* (16,214; credible interval = 1,254 to 70,584)
 347 divergence point estimates; the latter is about 1.6 times as large as the value in Turelli et al.
 348 (2018). (Nevertheless, the confidence intervals of our and Turelli et al. (2018)'s *wRi-wSuz*
 349 divergence estimates overlap.) To obtain an alternative estimate of *wNo-wMau* divergence, we
 350 estimated divergence time using the observed third-position pairwise divergence (0.077%, or
 351 0.039% from tip to MRCA) and Richardson et al. (2012)'s estimate of the "short-term
 352 evolutionary rate" of *Wolbachia* third-position divergence within *wMel*. This approach produces
 353 a point estimate of 57,000 years, with a credible interval of 30,000 to 135,000 years for the *wNo-*
 354 *wMau* split. In Cooper et al. (2019), we address in detail how a constant substitution-rate ratio
 355 among codon positions across the tree, assumed by the model, affects these estimates.

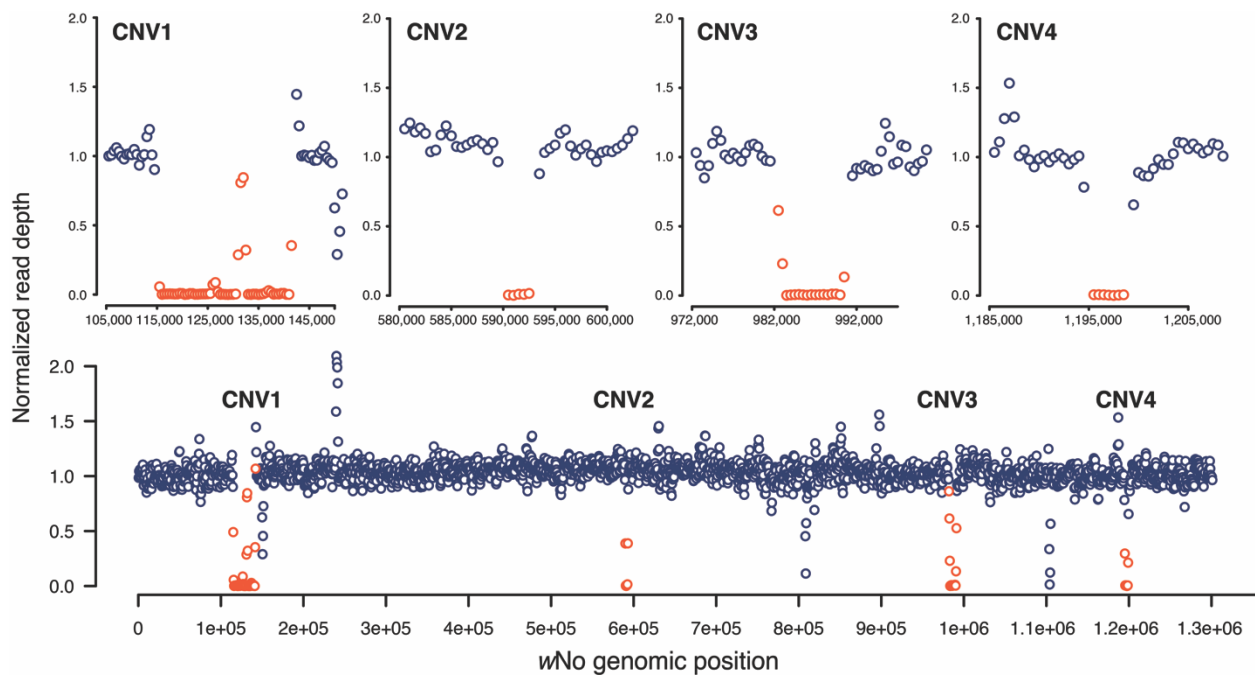


356
 357 **Figure 1. A)** An estimated phylogram for various group-A (red) and group-B (blue) *Wolbachia*
 358 strains. All nodes have Bayesian posterior probabilities of 1. The phylogram shows significant
 359 variation in the substitution rates across branches, with long branches separating the A and B
 360 clades. **B)** An estimated chronogram for the same strains, with estimated divergence times and
 361 their confidence intervals at each node. To obtain these estimates, we generated a relative
 362 relaxed-clock chronogram with the GTR + Γ model with the root age fixed to 1, the data
 363 partitioned by codon position, and with a $\Gamma(2,2)$ branch rate prior. We used substitution-rate
 364 estimates of $\Gamma(7,7) \times 6.87 \times 10^{-9}$ substitutions/3rd position site/year to transform the relative
 365 chronogram into an absolute chronogram.

366 **Analysis of *Wolbachia* and mitochondrial genomes**

367 We looked for CNVs in *w*Mau relative to sister *w*No by plotting normalized read depth along the
368 *w*No genome. There were no differences in copy number among the *w*Mau variants, but
369 compared to *w*No, ControlFREEEC identified four regions deleted from all *w*Mau that were
370 significant according to the Wilcoxon Rank Sum and Kolmogorov-Smirnov tests (Figure 2 and
371 Supplemental Table 3). These deleted regions of the *w*Mau genomes include many genes,
372 including many phage-related loci, providing interesting candidates for future work (listed in
373 Supplementary Table 4).

374



375

376 **Figure 2.** All *w*Mau variants share four large deletions, relative to sister *w*No. Top panel) The
377 normalized read depth for *w*Mau *R60* plotted across the four focal regions of the *w*No reference
378 genome; 10 kb of sequence surrounding regions are plotted on either side of each region. Bottom
379 panel) The normalized read depth of *w*Mau *R60* plotted across the whole *w*No reference genome.
380 Regions that do not contain statistically significant CNVs are plotted in dark blue, and regions
381 with significant CNVs are plotted in red. All *w*Mau variants share the same CNVs, relative to
382 *w*No.

383

384 To test the hypothesis that *cif* loci are disrupted, we searched for pairs of loci known to be
385 associated with CI and found homologs to the *cinA-cinB*^{*w*No} pair in each of our draft assemblies,
386 but we did not find homologs to the *cidA-cidB*^{*w*Me1}, *cidA-cidB*^{*w*Pip}, or to the *cinA-cinB*^{*w*Pip} pairs.
387 There were no variable sites in *cinA-cinB*^{*w*No} homologs among our five *w*Mau assemblies.

388 Relative to *wNo*, all *wMau* variants share a one base pair deletion at base 1133 out of 2091
389 (amino acid 378) in the *cinB^{wNo}* homolog. This frameshift introduces over 10 stop codons, with
390 the first at amino acid 388, potentially making this predicted CI-causing-toxin protein
391 nonfunctional. We also identified a nonsynonymous substitution in amino acid 264 of the
392 *cinB^{wNo}* homolog (*wNo* codon ACA, Thr; *wMau* codon AUA, Ile) and two SNVs in the region
393 homologous to *cinA^{wNo}*: a synonymous substitution in amino acid 365 (*wNo* codon GUC, *wMau*
394 codon GUU) and a nonsynonymous substitution in amino acid 397 (*wNo* codon GCU, amino
395 acid Ala; *wMau* codon GAU, amino acid Asp). Disruption of CI is consistent with theoretical
396 analyses showing that selection within a host species does not act directly on the level of CI
397 (Prout 1994; Turelli 1994; Haygood and Turelli 2009). Future functional analyses will determine
398 whether disruption of regions homologous to *cinA-cinB^{wNo}* underlie the lack of *wMau* CI.

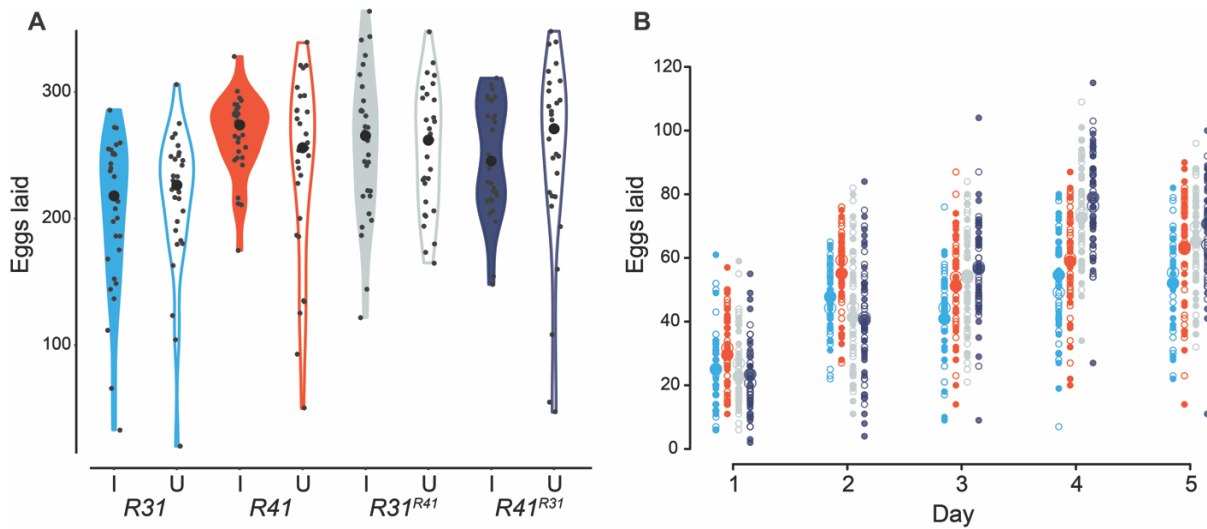
399 Of the *D. mauritiana* lines tested ($N = 9$), one line (uninfected-*R44*) carries the *maII*
400 mitochondrial haplotype, while the other eight carry *maI*. Rousset and Solignac (1995) reported a
401 similar *maII* frequency, with 3 of 26 lines sampled in 1985 carrying *maII*. The *maI* and *maII*
402 references differ by 343 SNVs across the proteome, and *R44* differs from the *maII* reference by 4
403 SNVs in the proteome. Four of our *maI* lines (*R23*, *R29*, *R32*, and *R39*) are identical to the *maI*
404 reference, while three (*R31*, *R41*, and *R60*) have one SNV and one (*R9*) has two SNVs relative to
405 *maI* reference. One SNV is shared between *R9* and *R60*, but the other three SNVs are unique.
406 Our results agree with past analyses that found *wMau* is perfectly associated with the *maI*
407 mitochondrial haplotype (Rousset and Solignac 1995; Ballard 2000a; James and Ballard 2000).
408 The presence of *maII* among the uninfected is interesting. In contrast to *maI*, which is associated
409 with introgression with *D. simulans* (Ballard 2000a; James and Ballard 2000), *maII* appears as an
410 outgroup on the mtDNA phylogeny of the *D. simulans* clade and is not associated with
411 *Wolbachia* (Ballard 2000b, Fig. 5; James and Ballard 2000). Whether or not *Wolbachia* cause CI,
412 if they are maintained by selection-imperfect-transmission balance, we expect all uninfected flies
413 to eventually carry the mtDNA associated with infected mothers (Turelli et al. 1992). We present
414 a mathematical analysis of the persistence of *maII* below.

415

416 **Analysis of *wMau* phenotypes**

417 In agreement with Giordano et al. (1995), we found no difference between the egg hatch of
418 uninfected females crossed to *wMau*-infected males (0.34 ± 0.23 SD, $N = 25$) and the reciprocal

419 cross (0.29 ± 0.28 SD, $N = 24$), indicating no CI. In contrast to Fast et al. (2011), we find no
 420 evidence that *w*Mau affects *D. mauritiana* fecundity (Supplemental Table 5 and Figure 3),
 421 regardless of host genetic backgrounds. Across both experiments assessing *w*Mau fecundity
 422 effects in their natural backgrounds (*R31* and *R41*), we counted 27,221 eggs and found no
 423 difference in the number of eggs laid by infected (mean = 238.20, SD = 52.35, $N = 60$) versus
 424 uninfected (mean = 226.82, SD = 67.21, $N = 57$) females over the five days of egg lay (Wilcoxon
 425 test, $W = 1540.5$, $P = 0.357$); and across both experiments that assessed *w*Mau fecundity effects
 426 in novel host backgrounds (*R31^{R41}* and *R41^{R31}*), we counted 30,358 eggs and found no difference
 427 in the number of eggs laid by infected (mean = 253.30, SD = 51.99, $N = 60$) versus uninfected
 428 (mean = 252.67, SD = 63.53, $N = 60$) females over five days (Wilcoxon test, $W = 1869.5$, $P =$
 429 0.719). [The mean number of eggs laid over five days, standard deviation (SD), sample size (N),
 430 and P -values from Wilcoxon tests are presented in Supplemental Table 5 for all pairs.]
 431

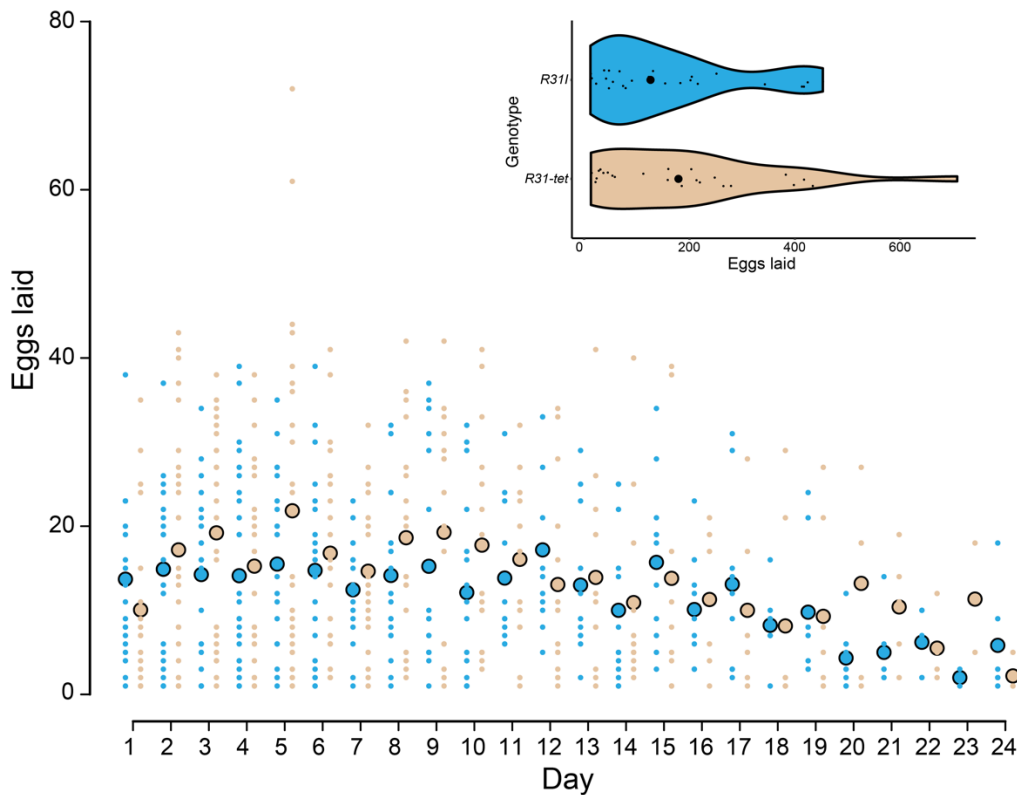


432
 433 **Figure 3.** *w*Mau infections do not influence *D. mauritiana* fecundity, regardless of host genomic
 434 background. **A)** Violin plots of the number of eggs laid by *D. mauritiana* females over five days
 435 when infected with their natural *w*Mau variant (*R31I* and *R41I*), when infected with a novel
 436 *w*Mau variant (*R31^{R41}I* and *R41^{R31}I*), and when uninfected (*R31U*, *R41U*, *R31^{R41}U*, and
 437 *R41^{R31}U*). Large black dots are medians, and small black dots are the eggs laid by each replicate
 438 over five days. **B)** The daily egg lay of these same infected (solid circles) and uninfected (open
 439 circles) *R31* (aqua), *R41* (red), *R31^{R41}* (gray), and *R41^{R31}* (dark blue) genotypes is reported. Large
 440 circles are means of all replicates, and small circles are the raw data. Only days where females
 441 laid at least one egg are plotted. Cytoplasm sources are denoted by superscripts for the
 442 reciprocally introgressed strains.

443
 444

445 We sought to determine if w Mau fecundity effects depend on host age with a separate
446 experiment that assessed egg lay over 24 days on apple-agar plates, similar to Fast et al. (2011).
447 Across all ages, we counted 9,459 eggs and found no difference in the number of eggs laid by
448 infected (mean = 156.29, SD = 138.04, $N = 28$) versus uninfected (mean = 187.70, SD = 168.28,
449 $N = 27$) females (Wilcoxon test, $W = 409$, $P = 0.608$) (Figure 4). While our point estimates
450 indicate that w Mau does not increase host fecundity, egg lay was generally lower and more
451 variable on agar plates relative to our analyses of egg lay on spoons described above.

452
453
454



455
456 **Figure 4.** The mean number of eggs laid by infected *R31* (*R31I*, large aqua dots) and uninfected
457 *R31-tet* (large tan dots) genotypes are similar. Egg counts for each replicate are also plotted
458 (small dots). Violin plots show egg lay across all ages for each genotype; large black circles are
459 medians, and small black circles are the number of eggs laid by each replicate.

460
461

462 With these data, we estimated the fitness parameter F in the standard discrete-generation
463 model of CI (Hoffmann et al. 1990; Turelli 1994). Taking the ratio of replicate mean fecundity

464 observed for *w*Mau-infected females to the replicate mean fecundity of uninfected females in
 465 naturally sampled *R31* and *R41 D. mauritiana* backgrounds, we estimated $F = 1.05$ (95% BC_a
 466 interval: 0.96, 1.16). Following reciprocal introgression of *w*Mau and host backgrounds (i.e., the
 467 *R31^{R41}* and *R41^{R31}* genotypes), we estimated $F = 1.0$ (95% BC_a interval: 0.93, 1.09). Finally,
 468 across all 24 days of our age-effects experiment, we estimated $F = 0.83$, 95% BC_a interval: 0.52,
 469 1.32) for *R31*, which overlaps with our estimate of F for *R31* in our initial experiment (Table 1).
 470 BC_a confidence intervals were calculated using the two-sample acceleration constant given by
 471 equation 15.36 of Efron and Tibshirani (1993). (Estimates of F and the associated BC_a
 472 confidence intervals are reported in Table 1 for each genotype and condition.) Consistent with
 473 our other analyses, we find little evidence that *w*Mau significantly increases fecundity. However,
 474 our data do not have much statistical power to detect values of F on the order of 1.05, which may
 475 suffice to produce $F(1 - \mu) > 1$ and deterministic spread of *w*Mau from low frequencies. We
 476 present our power calculations in Figure 1B of the Supplementary Information.

477

Table 1. Estimates of the relative fitness parameter F indicate that *w*Mau fecundity effects are likely to be minimal.

<i>w</i> Mau variant/age class	F	95% BC _a interval
<i>R31</i>	0.988	(0.862, 1.137)
<i>R41</i>	1.107	(0.995, 1.265)
<i>R31^{R41}</i>	1.012	(0.911, 1.122)
<i>R41^{R31}</i>	0.992	(0.884, 1.143)
<i>R31</i> (across age)	0.833	(0.515, 1.323)

478

479

480 Finally, we assessed the fidelity of *w*Mau maternal transmission under standard laboratory
 481 conditions. We excluded sublines that produced fewer than 8 F1 offspring. In all cases, *R31* ($N =$
 482 17) sublines produced offspring that were all infected, indicating perfect maternal transmission.
 483 In contrast, one *R41* subline produced one uninfected individual out of a total of 18 F1 offspring
 484 produced; all other *R41* sublines meeting our criteria ($N = 15$) produced only infected F1
 485 offspring, resulting in nearly perfect maternal transmission across all *R41* sublines ($\mu = 0.0039$).

486

487

488 **Mathematical analyses of *Wolbachia* frequencies and mtDNA polymorphism**

489 If *Wolbachia* do not cause CI (or any other reproductive manipulation), their dynamics can be
490 approximated by a discrete-generation haploid selection model. Following Hoffmann and Turelli
491 (1997), we assume that the relative fecundity of *Wolbachia*-infected females is F , but a fraction
492 μ of their ova do not carry *Wolbachia*. Given our ignorance of the nature of *Wolbachia*'s
493 favorable effects, the F represents an approximation for all fitness benefits. If $F(1 - \mu) > 1$, the
494 equilibrium *Wolbachia* frequency among adults is

495
496
$$\hat{p} = 1 - \frac{\mu F}{F - 1}. \quad (1)$$

497
498 Imperfect maternal transmission has been documented for field-collected *D. simulans* infected
499 with w_{Ri} (Hoffmann and Turelli 1988; Turelli and Hoffmann 1995; Carrington et al. 2011), *D.*
500 *melanogaster* infected with w_{Mel} (Hoffmann et al. 1998) and *D. suzukii* infected with w_{Suz}
501 (Hamm et al. 2014). The estimates range from about 0.01 to 0.1. Given that we have documented
502 imperfect maternal transmission of w_{Mau} in the laboratory, we expect (more) imperfect
503 transmission in nature (Turelli and Hoffmann 1995; Carrington et al. 2011). In order for the
504 equilibrium *Wolbachia* frequency to be below 0.5, approximation (1) requires that the relative
505 fecundity of infected females satisfies

506
507
$$F < \frac{1}{1 - 2\mu}. \quad (2)$$

508
509 Thus, even for μ as large as 0.15, which greatly exceeds our laboratory estimates for w_{Mau} and
510 essentially all estimates of maternal transmission failure from nature, *Wolbachia* can increase
511 fitness by at most 43% and produce an equilibrium frequency below 0.5 (Supplemental Figure
512 1A). Conversely, (1) implies that a doubling of relative fecundity by *Wolbachia* would produce
513 an equilibrium frequency $1 - 2\mu$. If $\mu \leq 0.25$, consistent with all available data, the predicted
514 equilibrium implied by a *Wolbachia*-induced fitness doubling significantly exceeds the observed
515 frequency of w_{Mau} . Hence, a four-fold fecundity effect, as described by Fast et al. (2011), is
516 inconsistent with the frequency of w_{Mau} in natural populations of *D. mauritiana*. Field estimates
517 of μ for *D. mauritiana* will provide better theory-based bounds on w_{Mau} fitness effects that

518 would be consistent with *w*Mau tending to increase when rare on Mauritius, i.e., conditions for
519 $F(1 - \mu) > 1$.

520 Our theoretical analysis, addressing the plausibility of a four-fold fitness increase caused by
521 *w*Mau, assumes that the observed frequency of *w*Mau approximates selection-transmission
522 equilibrium, as described by (1). With only two frequency estimates (one from a heterogeneous
523 collection of laboratory stocks), we do not know that the current low frequency is temporarily
524 stable. Also, we do not know that the mutations we detect in *cinA-cinB^{wNo}* homologs are
525 responsible for the lack of *w*Mau CI. One alternative is that *D. mauritiana* has evolved to
526 suppress CI (for host suppression of male killing, see Horne et al. 2006 and Vanthournout and
527 Hendrickx 2016). Host suppression of CI is expected (Turelli 1994), and it may explain the low
528 CI caused by *w*Mel in *D. melanogaster* (Hoffmann and Turelli 1997). However, the fact that
529 *w*Mau does not produce CI in *D. simulans*, a host that allows *w*Mel and other strains to induce
530 strong CI even though little CI is produced in their native hosts, argues against host suppression
531 as the explanation for the lack of CI caused by *w*Mau in *D. mauritiana*. Nevertheless, the loss of
532 CI from *w*Mau may be quite recent; and *w*Mau may be on its way to elimination in *D.*
533 *mauritiana*. If so, our equilibrium analysis is irrelevant – but this gradual-loss scenario is equally
534 inconsistent with the four-fold fecundity effect proposed by Fast et al. (2011).

535 As noted by Turelli et al. (1992), if *Wolbachia* is introduced into a population along with a
536 diagnostic mtDNA haplotype that has no effect on fitness, imperfect *Wolbachia* maternal
537 transmission implies that all infected and uninfected individuals will eventually carry the
538 *Wolbachia*-associated mtDNA, because all will have had *Wolbachia*-infected maternal ancestors.
539 We conjectured that a stable mtDNA polymorphism might be maintained if *Wolbachia*-
540 associated mtDNA introduced by introgression is deleterious in its new nuclear background. We
541 refute our conjecture in Appendix 1. We show that the condition for *Wolbachia* to increase when
542 rare, $F(1 - \mu) > 1$, ensures that the native mtDNA will be completely displaced by the
543 *Wolbachia*-associated mtDNA, even if it lowers host fitness once separated from *Wolbachia*.

544 How fast is the mtDNA turnover, among *Wolbachia*-uninfected individuals, as a new
545 *Wolbachia* invades? This is easiest to analyze when the mtDNA introduced with *Wolbachia* has
546 no effect on fitness, so that the relative fitness of *Wolbachia*-infected versus uninfected
547 individuals is F , irrespective of the mtDNA haplotype of the uninfected individuals. As shown in

548 Appendix 1, the frequency of the ancestral mtDNA haplotype among uninfected individuals,
549 denoted r_t , declines as

550

$$551 \quad r_{t+1} = r_t/[F(1 - \mu)]. \quad (3)$$

552

553 Assuming $r_0 = 1$, recursion (3) implies that even if $F(1 - \mu)$ is only 1.01, the frequency of the
554 ancestral mtDNA haplotype should fall below 10^{-4} after 1000 generations. A much more rapid
555 mtDNA turnover was seen as the CI-causing wRi swept northward through California
556 populations of *D. simulans* (Turelli et al. 1992; Turelli and Hoffmann 1995). Thus, it is
557 theoretically unexpected, under this simple model, that mtDNA haplotype *maII*, which seems to
558 be ancestral in *D. mauritiana* (Rousset and Solignac 1995; Ballard 2000a), persists among
559 *Wolbachia*-uninfected *D. mauritiana*, given that all sampled *Wolbachia*-infected individuals
560 carry *maI*. However, spatial variation in fitnesses is one possible explanation for this
561 polymorphism (Gliddon and Strobeck 1975), which has persisted since at least 1985.

562

563 **DISCUSSION**

564 ***wMau* is sister to *wNo* and diverged from group-A *Wolbachia* less than 100 mya**

565 Our phylogenetic analyses place *wMau* sister to *wNo*, in agreement with past analyses using
566 fewer data (James and Ballard 2000; Zabalou et al. 2008; Toomey et al. 2013). The relationships
567 we infer agree with those from recently published phylograms (Gerth and Bleidorn 2016;
568 Lindsey et al. 2018) (Figure 1A).

569 Depending on the prior used for substitution-rate variation, we estimate that *wMau* and other
570 group-B *Wolbachia* diverged from group-A strains about 6–46 mya. This is roughly consistent
571 with a prior estimate using only *ftsZ* (58–67 mya, Werren et al. 1995), but is inconsistent with a
572 recent estimate using 179,763 bases across 252 loci (76–460 mya, Gerth and Bleidorn 2016).
573 There are several reasons why we question the Gerth and Bleidorn (2016) calibration. First,
574 Gerth and Bleidorn (2016)'s chronogram placed *wNo* sister to all other group-B *Wolbachia*, in
575 disagreement with their own phylogram (Gerth and Bleidorn 2016, Figure 3). In contrast, our
576 phylogram and that of Lindsey et al. (2018) support *wAlbB* splitting from all other strains at this
577 node. Second, the Gerth and Bleidorn (2016) calibration estimated the split between *wRi* that
578 infects *D. simulans* and *wSuz* that infects *D. sukukii* at 900,000 years. This estimate is more than

579 an order of magnitude higher than ours (16,214 years) and nearly two orders of magnitude higher
580 than the 11,000 year estimate of Turelli et al. (2018) who found 0.014% third position
581 divergence between *w*Ri and *w*Suz (i.e., 0.007% along each branch) over 506,307 bases.
582 Raychoudhury et al. (2009) and Richardson et al. (2012) both estimated a rate of about 7×10^{-9}
583 substitutions/3rd position site/year between *Wolbachia* in *Nasonia* wasps and within *w*Mel,
584 respectively. An estimate of 900,000 years requires a rate about 100 times slower, 7.8×10^{-11}
585 substitutions/3rd position site/year, which seems implausible. Finally, using data kindly provided
586 by Michael Gerth, additional analyses indicate that the third-position rates required for the
587 *Wolbachia* divergence times estimated by Gerth and Bleidorn (2016) between *Nomada flava* and
588 *N. leucophthalma* (1.72×10^{-10}), *N. flava* and *N. panzeri* (3.78×10^{-10}) (their calibration point),
589 and *N. flava* and *N. ferruginata* (4.14×10^{-10}) are each more than 10 times slower than those
590 estimated by Raychoudhury et al. (2009) and Richardson et al. (2012), which seems unlikely.
591 Our analyses suggest that the A-B group split occurred less than 100 mya.

592

593 **The lack of CI is consistent with intermediate *w*Mau infection frequencies**

594 Across 671 genes (682,494 bases), the *w*Mau genomes were identical and differed from *w*No by
595 only 0.068%. Across the coding regions we analyzed, we found few SNVs and no CNVs among
596 *w*Mau variants. Our analyses did identify four large deletions shared by all *w*Mau genomes,
597 relative to *w*No. Despite the close relationship between *w*Mau and *w*No, *w*No causes CI while
598 *w*Mau does not (Giordano et al. 1995; Merçot et al. 1995; Rousset and Solignac 1995, our data).
599 We searched for all pairs of loci known to cause CI and found only homologs to the *cinA*-
600 *cinB*^{*w*No} pair in *w*Mau genomes. All *w*Mau variants share a one-base-pair deletion in the *w*Mau
601 region homologous to *cinB*^{*w*No}. This mutation introduces a frameshift and more than ten stop
602 codons. Future functional work will help determine if disruption of this predicted-toxin locus
603 underlies the lack of CI in *w*Mau. Regardless, the lack of CI is consistent with the prediction that
604 selection within host lineages does not directly act on the intensity of CI (Prout 1994; Turelli
605 1994). We predict that analysis of additional non-CI-causing strains will reveal additional
606 examples of genomic remnants of CI loci. Among non-CI *Wolbachia*, the relative frequency of
607 those with non-functional CI loci, versus no CI loci, is unknown.

608 Irrespective of whether CI was lost or never gained, non-CI *Wolbachia* have lower expected
609 equilibrium infection frequencies than do CI-causing variants (Kriesner et al. 2016). The *w*Mau

610 infection frequency of approximately 0.34 on Mauritius (Giordano et al. 1995; our data) is
611 consistent with this prediction. Additional sampling of Mauritius, preferably over decades, will
612 determine whether intermediate *w*Mau frequencies are temporally stable. Such temporal stability
613 depends greatly on values of F and μ through time suggesting additional field-based estimates of
614 these parameters will be useful.

615 *w*Mau co-occurs with essentially the same mitochondrial haplotype as *w*Ma that infects *D.*
616 *simulans* on Madagascar and elsewhere in Africa and the South Pacific (Rousset and Solignac
617 1995; Merçot and Poinot 1998; Ballard 2000a; James and Ballard 2000; James et al. 2002;
618 Ballard 2004), suggesting that *w*Mau and *w*Ma may be the same strain infecting different host
619 species following introgressive *Wolbachia* transfer (see below). *w*Mau and *w*Ma phenotypes are
620 also more similar to one another than to *w*No, with only certain crosses between *w*Ma-infected
621 *D. simulans* males and uninfected *D. simulans* females inducing CI (James and Ballard 2000).
622 Polymorphism in the strength of CI induced by *w*Ma could result from host modification of
623 *Wolbachia*-induced CI (Reynolds and Hoffmann 2002; Cooper et al. 2017), or from *Wolbachia*
624 titer variation that influences the strength of CI and/or the strength of CI rescue by infected
625 females. Alternatively, the single-base-pair deletion in the *cinB*^{*w*No} homolog or other mutations
626 that influence CI strength, could be polymorphic in *w*Ma. *w*Ma infection frequencies in *D.*
627 *simulans* are intermediate on Madagascar (infection frequency = 0.25, binomial confidence
628 intervals: 0.14, 0.40; James and Ballard 2000), consistent with no CI, suggesting replication of
629 rarely observed *w*Ma CI is needed. Including *D. simulans* from the island of Réunion in this
630 infection-frequency further supports the conjecture that *w*Ma causes little or no CI (infection
631 frequency = 0.31, binomial confidence intervals: 0.20, 0.45; James and Ballard 2000).
632 Unfortunately, no Madagascar *D. simulans* stocks available at the National *Drosophila* Species
633 Stock Center were *w*Ma infected, precluding detailed analysis of this strain.

634 Our genomic data indicate that *w*Mau may maintain an ability to rescue CI, as the *cinA*^{*w*No}
635 homolog is intact in *w*Mau genomes with only one nonsynonymous substitution relative to
636 *cinA*^{*w*No}; *cidA* in *w*Mel was recently shown to underlie transgenic-CI rescue (Shropshire et al.
637 2018). *w*Ma seems to sometimes rescue CI, but conflicting patterns have been found, and
638 additional experiments are needed to resolve this (Rousset and Solignac 1995; Bourtzis et al.
639 1998; Merçot and Poinot 1998; James and Ballard 2000; Merçot and Poinot 2003; Zabalou et
640 al. 2008). Future work that tests for CI rescue by *w*Mau and *w*Ma-infected females crossed with

641 males infected with *w*No or other CI-causing strains, combined with genomic analysis of CI loci
642 in *w*Ma, will be useful.

643

644 ***w*Mau does not influence *D. mauritiana* fecundity**

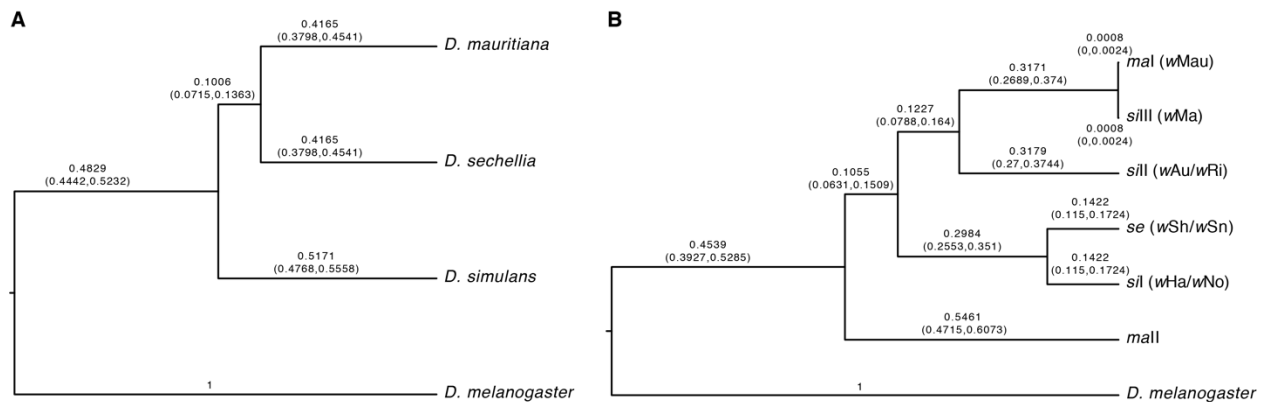
645 While selection does not directly act on the level of CI (Prout 1994; Turelli 1994; Haygood and
646 Turelli 2009), it does act to increase the product *Wolbachia*-infected host fitness and the
647 efficiency of maternal transmission (Turelli 1994). Understanding the *Wolbachia* effects that
648 lead to spread from low frequencies and the persistence of non-CI causing *Wolbachia* at
649 intermediate frequencies is crucial to explaining *Wolbachia* prevalence among insects and other
650 arthropods. The four-fold fecundity effect of *w*Mau reported by Fast et al. (2011) in *D.*
651 *mauritiana* is inconsistent with our experiments and with the intermediate infection frequencies
652 observed in nature. We find no *w*Mau effects on host fecundity, regardless of host background,
653 with our estimates of *F* having BCa intervals that include 1. Small increases in *F* could allow the
654 deterministic spread of *w*Mau from low frequencies, although detecting very small increases in *F*
655 is difficult (Supplemental Figure 1B). Our results are consistent with an earlier analysis that
656 assessed egg lay of a single genotype and found no effect of *w*Mau on host fecundity (Giordano
657 et al. 1995). When combined with the low observed infection frequencies, our fecundity data are
658 also consistent with our mathematical analyses indicating that *Wolbachia* can increase host
659 fitness by at most about 50% for reasonable estimates of μ . Because fecundity is one of many
660 fitness components, analysis of other candidate phenotypes for aiding the spread of low-
661 frequency *Wolbachia* is needed.

662

663 **Introgressive *Wolbachia* transfer likely predominates in the *D. simulans* clade**

664 Hybridization and introgression in the *D. simulans* clade may have led to introgressive transfer
665 of *Wolbachia* among host species (Rousset and Solignac 1995). This has been observed in other
666 *Drosophila* (Turelli et al. 2018; Cooper et al. 2019) and *Nasonia* wasps (Raychoudhury et al.
667 2009). The number of *Wolbachia* strains in the *D. simulans* clade, and the diversity of
668 mitochondria they co-occur with, is complex. Figure 5A shows host relationships and Figure 5B
669 shows mitochondrial relationships, with co-occurring *Wolbachia* variants in parentheses. While
670 *D. mauritiana* is singly infected by *w*Mau, *D. simulans* is infected by several strains, including
671 CI-causing *w*Ha and *w*No that often co-occur as double infections within individuals (O'Neill

672 and Karr 1990; Merçot et al. 1995; Rousset and Solignac 1995). *w*Ha and *w*No are similar to
 673 *w*Sh and *w*Sn, respectively, that infect *D. sechellia* (Giordano et al. 1995; Rousset and Solignac
 674 1995). *w*Ha and *w*Sh also occur as single infections in *D. simulans* and in *D. sechellia*,
 675 respectively (Rousset and Solignac 1995). In contrast, *w*No almost always co-occurs with *w*Ha in
 676 doubly infected *D. simulans* individuals (James et al. 2002), and *w*Sn seems to occur only with
 677 *w*Sh (Rousset and Solignac 1995). *D. simulans* has three distinct mitochondrial haplotypes (*si*I,
 678 *si*II, *si*III) associated with *w*Au/*w*Ri (*si*II), *w*Ha/*w*No (*si*I), and *w*Ma (*si*III). The *si*I haplotype is
 679 closely related to the *se* haplotype found with *w*Sh and *w*Sn in *D. sechellia* (Ballard 2000b). *w*Ma
 680 co-occurs with the *si*III haplotype, which differs over its 13 protein-coding genes by only a
 681 single-base pair from the *ma*I mitochondrial haplotype carried by *w*Mau-infected *D. mauritiana*.
 682 A second haplotype (*ma*II) is carried by only uninfected *D. mauritiana* (Ballard 2000a; James
 683 and Ballard 2000).
 684



685 **Figure 5. A)** A nuclear relative chronogram. **B)** A mitochondrial relative chronogram with co-
 686 occurring *Wolbachia* strains listed in parentheses. See the text for an interpretation of the results,
 687 including the artifactual resolution of the phylogeny of the *D. simulans* clade.
 688
 689

690
 691 The lack of whole *w*Ma genome data precludes us from confidently resolving the mode of
 692 *w*Mau acquisition in *D. mauritiana*. However, mitochondrial relationships support the proposal
 693 of Ballard (2000b) that *D. mauritiana* acquired *w*Mau and the *ma*I mitochondrial haplotype via
 694 introgression from *w*Ma-infected *D. simulans* carrying *si*III. *D. mauritiana* mitochondria are
 695 paraphyletic relative to *D. sechellia* and *D. simulans* mitochondria (Solignac and Monnerot
 696 1986; Satta and Takahata 1990; Ballard 2000a, 2000b), with *ma*I sister to *si*III and *ma*II outgroup
 697 to all other *D. simulans*-clade haplotypes (see Figure 5). Of the nine genomes we assessed, all

698 but one (uninfected-*R44*) carry the *maI* haplotype, and genotypes carrying *maI* are both *wMau*-
699 infected ($N = 5$) and uninfected ($N = 3$). While *wMa*-infected *D. simulans* carry *siIII*, *wNo*-
700 infected *D. simulans* carry *siI*. We estimate that *wMau* and *wNo* diverged about 55,000 years
701 ago, with only 0.068% sequence divergence over 682,494 bp. Nevertheless, it seems implausible
702 that *wNo* (versus *wMa*) was transferred directly to *D. mauritiana* as this requires horizontal or
703 paternal transmission of *wNo* into a *D. mauritiana* background already carrying the *maI*
704 mitochondrial haplotype. Although our nuclear result suggests a confident phylogenetic
705 resolution of the *D. simulans* clade (Figure 5A), this is an artifact of the bifurcation structure
706 imposed by the phylogenetic analysis. Population genetic analyses show a complex history of
707 introgression and probable shared ancestral polymorphisms (Kliman et al. 2000) among these
708 three species. Consistent with this, of the 20 nuclear loci we examined, 6 (*aconitase*, *aldolase*,
709 *bicoid*, *ebony*, *enolase*, *ninaE*) supported *D. mauritiana* as the outgroup within the *D. simulans*
710 clade, 7 (*glyp*, *pepck*, *pgm*, *pic*, *ptc*, *transaldolase*, *wingless*) supported *D. sechellia* as the
711 outgroup, and 7 (*esc*, *g6pdh*, *glys*, *pgi*, *tpi*, *white*, *yellow*) supported *D. simulans*. With successive
712 invasions of the islands and purely allopatric speciation, we expect the outgroup to be the island
713 endemic that diverged first. Figure 5B indicates that the *maII* haplotype diverged from the other
714 mtDNA haplotypes roughly when the clade diverged, with the other haplotypes subject to a
715 complex history of introgression and *Wolbachia*-associated sweeps, as described by Ballard
716 (2000b).

717 Ballard (2000b) estimated that *siIII-maI* diverged about 4,500 years ago, which presumably
718 approximates the date of the acquisition of *wMau* (and *siIII*, which became *maI*) by *D.*
719 *mauritiana*. This is surely many thousands of generations given previous estimates that consider
720 the temperature dependence of *Drosophila* development (Cooper et al. 2014; Cooper et al. 2018).
721 As shown by our mathematical analyses (Eq. 3), the apparent persistence of the *maII* mtDNA
722 among *Wolbachia*-uninfected *D. mauritiana*—without its occurrence among infected
723 individuals—is unexpected. More extensive sampling of natural *D. mauritiana* populations is
724 needed to see if this unexpected pattern persists. The persistence of this haplotype is inconsistent
725 with simple null models, possibly indicating interesting fitness effects.

726 While paternal transmission has been observed in *D. simulans* (Hoffmann and Turelli 1988;
727 Turelli and Hoffmann 1995), it seems to be very rare (Richardson et al. 2012; Turelli et al.
728 2018). *wNo* almost always occurs in *D. simulans* individuals also infected with *wHa*,

729 complicating this scenario further. It is possible that horizontal or paternal transmission of *w*Ma
730 or *w*No between *D. simulans* backgrounds carrying different mitochondrial haplotypes underlies
731 the similarities of these strains within *D. simulans*, despite their co-occurrence with distinct
732 mitochondria. Given the diversity of *Wolbachia* that infect *D. simulans*-clade hosts, and known
733 patterns of hybridization and introgression among hosts (Garrigan et al. 2012; Brand et al. 2013;
734 Garrigan et al. 2014; Matute and Ayroles 2014; Schrider et al. 2018), determining relationships
735 among these *Wolbachia* and how *D. mauritiana* acquired *w*Mau will require detailed
736 phylogenomic analysis of nuclear, mitochondrial, and *Wolbachia* genomes in the *D. simulans*
737 clade.

738

739 **AUTHOR CONTRIBUTIONS**

740 MM performed the molecular and phenotypic work, participated in the design of the study, and
741 contributed to the writing; WC performed the phylogenetic and genomic analyses and
742 contributed to the writing; SR contributed to the molecular and phenotypic analyses and to the
743 writing; JB performed the library preparation and contributed to the writing; MT contributed to
744 the analyses, data interpretation, and writing; BSC designed and coordinated the study,
745 contributed to the analyses and data interpretation, and drafted the manuscript. All authors gave
746 final approval for publication.

747

748 **ACKNOWLEDGMENTS**

749 We thank Margarita Womack for sampling the *D. mauritiana* used in this study and Daniel
750 Matute for sharing them. We thank Michael Gerth for sharing *Nomada* genomic data. Isaac
751 Humble, Maria Kirby, and Tim Wheeler assisted with data collection. Michael Gerth, Michael
752 Hague, and Amelia Lindsey provided comments that improved earlier drafts of this manuscript.
753 Computational resources were provided by the University of Montana Genomics Core. Research
754 reported in this publication was supported by the National Institute Of General Medical Sciences
755 of the National Institutes of Health (NIH) under Award Number R35GM124701 to B.S.C. The
756 content is solely the responsibility of the authors and does not necessarily represent the official
757 views of the NIH. The authors declare no conflicts of interest.

758

759

760 **LITERATURE CITED**

- 761 Baldo, L., N. A. Ayoub, C. Y. Hayashi, J. A. Russell, J. K. Stahlhut, and J. H. Werren. 2008
762 Insight into the routes of *Wolbachia* invasion: high levels of horizontal transfer in the
763 spider genus *Agelenopsis* revealed by *Wolbachia* strain and mitochondrial DNA
764 diversity. *Molecular Ecology* 17:557–569.
- 765 Ballard, J. W. O. 2000a. When one is not enough: introgression of mitochondrial DNA in
766 *Drosophila*. *Molecular Biology and Evolution* 17:1126–1130.
- 767 Ballard, J. W. 2000b. Comparative genomics of mitochondrial DNA in *Drosophila simulans*.
768 *Journal of Molecular Evolution* 51:64–75.
- 769 Ballard, J. W. O. 2004. Sequential evolution of a symbiont inferred from the host: *Wolbachia*
770 and *Drosophila simulans*. *Molecular Biology and Evolution* 21:428–442.
- 771 Ballard, J. W., and R. G. Melvin. 2007. Tetracycline treatment influences mitochondrial
772 metabolism and mtDNA density two generations after treatment in *Drosophila*. *Insect*
773 *Molecular Biology* 16:799–802.
- 774 Barton, N. H., and M. Turelli. 2011. Spatial waves of advance with bistable dynamics:
775 cytoplasmic and genetic analogues of allee effects. *American Naturalist* 178:E48–E75.
- 776 Beckmann, J. F., and A. M. Fallon. 2013. Detection of the *Wolbachia* protein WPIP0282 in
777 mosquito spermathecae: implications for cytoplasmic incompatibility. *Insect*
778 *Biochemistry and Molecular Biology* 43:867–878.
- 779 Beckmann, J. F., J. A. Ronau and M. Hochstrasser. 2017. A *Wolbachia* deubiquitylating enzyme
780 induces cytoplasmic incompatibility. *Nature Microbiology* 2:17007.
- 781 Beckmann, J. F., M. Bonneau, H. Chen, M. Hochstrasser, D. Poinso, H. Merçot, M. Weill, M.
782 Sicard, and S. Charlat. 2019. The toxin-antidote model of cytoplasmic incompatibility:
783 genetics and evolutionary implications. *Trends in Genetics* in press.
- 784 Boeva, V., T. Popova, K. Bleakley, P. Chiche, J. Cappo, G. Schleiermacher, I. Janoueix-Lerosey,
785 O. Delattre, E. Barillot. 2012. Control-FREEC: a tool for assessing copy number and
786 allelic content using next-generation sequencing data. *Bioinformatics* 28:423–425.
- 787 Bourtzis, K., S. L. Dobson, H. R. Braig and S. L. O'Neill. 1998. Rescuing *Wolbachia* have been
788 overlooked. *Nature* 391:852–853.
- 789 Brand, C. L., S. B. Kingan, L. Wu and D. Garrigan. 2013. A Selective Sweep across Species
790 Boundaries in *Drosophila*. *Molecular Biology and Evolution* 30:2177–2186.
- 791 Brownlie, J. C., B. N. Cass, M. Riegler, J. J. Witsenburg, I. Iturbe-Ormaetxe, E. A. McGraw, S.
792 L. O'Neill. 2009. Evidence for Metabolic Provisioning by a Common Invertebrate
793 Endosymbiont, *Wolbachia pipientis*, during Periods of Nutritional Stress. *PLoS*
794 *Pathogens* 5:e1000368.
- 795 Carrington, L. B., J. R. Lipkowitz, A. A. Hoffmann, and M. Turelli. 2011. A re-examination of
796 *Wolbachia*-induced cytoplasmic incompatibility in California *Drosophila simulans*. *PLoS*
797 *ONE* 6:e22565
- 798 Caspari, E., and G. S. Watson. 1959. On the evolutionary importance of cytoplasmic sterility in
799 mosquitoes. *Evolution* 13:568–570.
- 800 Cattel, J., K. Nikolouli, T. Andrieux, J. Martinez, F. Jiggins, S. Charlat, F. Vavre, D. Lejon, P.
801 Gibert, and L. Mouton. 2018. Back and forth *Wolbachia* transfers reveal efficient strains
802 to control spotted wing *Drosophila* populations. *Journal of Applied Ecology* 55:2408-
803 2418.
- 804

805 Conner, W. R., M. L. Blaxter, G. Anfora, L. Ometto, O. Rota-Stabelli, and M. Turelli. 2017.
806 Genome comparisons indicate recent transfer of *w*Ri-like *Wolbachia* between sister
807 species *Drosophila suzukii* and *D. subpulchrella*. *Ecology and Evolution* 7:9391–9404.

808 Cooper, B. S., L. A. Hammad, and K. L. Montooth. 2014. Thermal adaptation of cellular
809 membranes in natural populations of *Drosophila melanogaster*. *Functional Ecology*.
810 28:886-894.

811 Cooper, B. S., P. S. Ginsberg, M. Turelli and D. R. Matute. 2017. *Wolbachia* in the *Drosophila*
812 *yakuba* complex: pervasive frequency variation and weak cytoplasmic incompatibility,
813 but no apparent effect on reproductive isolation. *Genetics* 205:333–351.

814 Cooper, B. S., A. Sedghifar, W. T. Nash, A. A. Comeault, D. R. Matute. 2018. A maladaptive
815 combination of traits contributes to the maintenance of a *Drosophila* hybrid zone. *Current*
816 *Biology*. 28:2940-2947.

817 Cooper, B. S., D. Vanderpool, W. R. Conner, D. R. Matute, and M. Turelli. 2019. Introgressive
818 and horizontal acquisition of *Wolbachia* by *Drosophila yakuba*-clade hosts and horizontal
819 transfer of incompatibility loci between distantly related *Wolbachia*. bioRxiv.
820 doi.org/10.1101/551036.

821 David, J., S. McEvey, M. Solignac and L. Tsacas. 1989. *Drosophila* communities on Mauritius
822 and the ecological niche of *D. mauritiana* (Diptera, Drosophilidae). *Revue De Zoologie*
823 *Africaine – Journal of African Zoology* 103:107–116.

824 Dean, M. D., and J. W. Ballard. 2004. Linking phylogenetics with population genetics to
825 reconstruct the geographic origin of a species. *Molecular Phylogenetics and Evolution*
826 32:998–1009.

827 Efron, B., and R. Tibshirani. 1993. *An Introduction to the Bootstrap*. Chapman & Hall, New
828 York, NY.

829 Ellegaard, K. M., L. Klasson, K. Näslund, K. Bourtzis and S. G. E. Andersson. 2013.
830 Comparative Genomics of *Wolbachia* and the Bacterial Species Concept. *PLoS Genetics*
831 9:e1003381.

832 Fast, E. M., M. E. Toomey, K. Panaram, D. Desjardins, E. D. Kolaczyk, H. M. Frydman. 2011.
833 *Wolbachia* enhance *Drosophila* stem cell proliferation and target the germline stem cell
834 niche. *Science* 334:990–992.

835 Fisher, R. A. 1937. The wave of advance of advantageous genes. *Annals of Eugenics* 7:355–369.

836 Garrigan, D., S. B. Kingan, A. J. Geneva, P. Andolfatto, A. G. Clark, K. R. Thornton, D. C.
837 Presgraves. 2012. Genome sequencing reveals complex speciation in the *Drosophila*
838 *simulans* clade. *Genome Research* 22:1499–1511.

839 Garrigan, D., S. B. Kingan, A. J. Geneva, J. P. Vedanayagam and D. C. Presgraves. 2014.
840 Genome diversity and divergence in *Drosophila mauritiana*: multiple signatures of faster
841 X evolution. *Genome Biology and Evolution* 6:2444–2458.

842 Gerth, M., and C. Bleidorn. 2016. Comparative genomics provides a timeframe for *Wolbachia*
843 evolution and exposes a recent biotin synthesis operon transfer. *Nature Microbiology*
844 2:16241.

845 Giordano, R., S. L. O'Neill and H. M. Robertson. 1995. *Wolbachia* infections and the expression
846 of cytoplasmic incompatibility in *Drosophila sechellia* and *D. mauritiana*. *Genetics*
847 140:1307–1317.

848 Gliddon, C. and C. Strobeck. 1975. Necessary and sufficient conditions for multiple-niche
849 polymorphism in haploids. *American Naturalist* 109:233–235.

850 Gloor, G. B., C. R. Preston, D. M. Johnsonschlitz, N. A. Nassif, R. W. Phillis, W. K. Benz, H.
851 M. Robertson, W. R. Engels. 1993. Type-1 repressors of P-element mobility. *Genetics*
852 135:81–95.

853 Gupta, V., R. B. Vasanthakrishnan, J. Siva-Jothy, K. M. Monteith, S. P. Brown, and P. F. Vale.
854 2017. The route of infection determines *Wolbachia* antibacterial protection in
855 *Drosophila*. *Proceedings of the Royal Society B: Biological Sciences* 284:20170809.

856 Hamm, C. A., D. J. Begun, A. Vo, C. C. R. Smith, P. Saelao, A. O. Shaver, J. Jaenike, M.
857 Turelli. 2014. *Wolbachia* do not live by reproductive manipulation alone: infection
858 polymorphism in *Drosophila suzukii* and *D. subpulchrella*. *Molecular Ecology* 23:4871–
859 4885.

860 Haygood, R., and M. Turelli. 2009. Evolution of incompatibility-inducing microbes in
861 subdivided host populations. *Evolution* 63:432–447

862 Hedges, L. M., J. C. Brownlie, S. L. O'Neill and K. N. Johnson. 2008. *Wolbachia* and virus
863 protection in insects. *Science* 322:702.

864 Hilgenboecker, K., P. Hammerstein, P. Schlattmann, A. Telschow and J. H. Werren. 2008. How
865 many species are infected with *Wolbachia*? A statistical analysis of current data. *FEMS*
866 *Microbiology Letters* 281:215–220.

867 Hoffmann, A. A., M. Turelli, and G. M. Simmons. 1986. Unidirectional incompatibility between
868 populations of *Drosophila simulans*. *Evolution* 40:692–701.

869 Hoffmann, A. A., and M. Turelli. 1988. Unidirectional incompatibility in *Drosophila simulans*:
870 Inheritance, geographic variation and fitness effects. *Genetics* 119:435–444.

871 Hoffmann, A. A., and M. Turelli. 1997. Cytoplasmic incompatibility in insects. In *Influential*
872 *passengers: inherited microorganisms and arthropod reproduction*, edited by S. L.
873 O'Neill, J. H. Werren, and A. A. Hoffmann. Oxford University Press, pp. 42–80.

874 Hoffmann, A. A., D. Clancy and J. Duncan. 1996. Naturally-occurring *Wolbachia* infection in
875 *Drosophila simulans* that does not cause cytoplasmic incompatibility. *Heredity* 76:1–8.

876 Hoffmann, A. A., M. Hercus and H. Dagher. 1998. Population dynamics of the *Wolbachia*
877 infection causing cytoplasmic incompatibility in *Drosophila melanogaster*. *Genetics*
878 148:221–231.

879 Hoffmann, A. A., M. Turelli, and L. G. Harshman. 1990. Factors affecting the distribution of
880 cytoplasmic incompatibility in *Drosophila simulans*. *Genetics* 126:933–948.

881 Hoffmann, A. A., B. L. Montgomery, J. Popovici, I. Iturbe-Ormaetxe, P. H. Johnson, F. Muzzi,
882 M. Greenfield, M. Durkan, Y. S. Leong, Y. Dong, H. Cook, J. Axford, A. G. Callahan, N.
883 Kenny, C. Omodei, E. A. McGraw, P. A. Ryan, S. A. Ritchie, M. Turelli, and S. L.
884 O'Neill. 2011. Successful establishment of *Wolbachia* in *Aedes* populations to suppress
885 dengue transmission. *Nature* 476:454–457.

886 Höhna, S., M. J. Landis, T. A. Heath, B. Boussau, N. Lartillot, B. R. Moore, J. P. Huelsenbeck,
887 F. Ronquist. 2016. RevBayes: Bayesian Phylogenetic Inference Using Graphical Models
888 and an Interactive Model-Specification Language. *Systematic Biology*. 65:726–736.

889 Hornett, E. A., S. Charlat, A. M. R. Duploux, N. Davies, G. K. Roderick, N. Wedell, and G. D.
890 D. Hurst. 2006. Evolution of male-killer suppression in a natural population. *PLoS*
891 *Biology* 4:e283.

892 Huigens, M. E., R. P. de Almeida, P. A. Boons, R. F. Luck and R. Stouthamer. 2004. Natural
893 interspecific and intraspecific horizontal transfer of parthenogenesis-inducing *Wolbachia*
894 in *Trichogramma* wasps. *Proceedings of the Royal Society B: Biological Sciences*
895 271:509–515.

896 Hurst, G. D. D. and F. M. Jiggins. 2000. Male-killing bacteria in insects: mechanisms, incidence,
897 and implications. *Emerging Infectious Diseases* 6:329-336.

898 Jackman, S. D., B. P. Vandervalk, H. Mohamadi, J. Chu, S. Yeo, S. A. Hammond, G. Jahesh, H.
899 Khan, L. Coombe, R. L. Warren, I. Birol. 2017. ABySS 2.0: resource-efficient assembly
900 of large genomes using a Bloom filter. *Genome Research* 27:768–777.

901 James, A. C., and J. W. O. Ballard. 2000. Expression of cytoplasmic incompatibility in
902 *Drosophila simulans* and its impact on infection frequencies and distribution of
903 *Wolbachia pipientis*. *Evolution* 54:1661–1672.

904 James, A. C., M. D. Dean, M. E. McMahon and J. W. Ballard. 2002. Dynamics of double and
905 single *Wolbachia* infections in *Drosophila simulans* from New Caledonia. *Heredity*
906 88:182–189.

907 Jeyaprakash, A., and M. A. Hoy. 2000. Long PCR improves *Wolbachia* DNA amplification: wsp
908 sequences found in 76% of sixty-three arthropod species. *Insect Molecular Biology*
909 9:393–405.

910 Joshi, N. A., and J. N. Fass. 2011. Sickle: A sliding-window, adaptive, quality-based trimming
911 tool for FastQ files (Version 1.33). Available at <https://github.com/najoshi/sickle>.

912 Katoh, K., and D. M. Standley. 2013. MAFFT Multiple Sequence Alignment Software Version
913 7: Improvements in Performance and Usability. *Molecular Biology and Evolution*
914 30:772–780.

915 Kent, B. N., L. Salichos, J. G. Gibbons, A. Rokas, I. L. Newton, M. E. Clark, S. R. Bordenstein.
916 2011. Complete bacteriophage transfer in a bacterial endosymbiont (*Wolbachia*)
917 determined by targeted genome capture. *Genome Biology and Evolution* 3:209–218.

918 Klasson, L., T. Walker, M. Sebahia, M. J. Sanders, M. A. Quail, A. Lord, S. Sanders, J. Earl, S.
919 L. O’Neill, N. Thomson, S. P. Sinkins, J. Parkhill. 2008. Genome evolution of *Wolbachia*
920 strain wPip from the *Culex pipiens* group. *Molecular Biology and Evolution* 25:1877–
921 1887.

922 Klasson, L., J. Westberg, P. Sapountzis, K. Näslund, Y. Lutnaes, A. C. Darby, Z. Veneti, L.
923 Chen, H. R. Braig, and R. Garrett. 2009. The mosaic genome structure of the *Wolbachia*
924 wRi strain infecting *Drosophila simulans*. *Proceedings of the National Academy of*
925 *Sciences* 106:5725–5730.

926 Kliman, R. M., P. Andolfatto, J. A. Coyne, F. Depaulis, M. Kreitman, A. J. Berry, J. McCarter, J.
927 Wakeley, and J. Hey. 2000. The population genetics of the origin and divergence of the
928 *Drosophila simulans* species complex. *Genetics* 156:1913–1931.

929 Kriesner, P., and A. A. Hoffmann. 2018. Rapid spread of a *Wolbachia* infection that does not
930 affect host reproduction in *Drosophila simulans* cage populations. *Evolution* 72:1475–
931 1487.

932 Kriesner, P., W. R. Conner, A. R. Weeks, M. Turelli, and A. A. Hoffmann. 2016. Persistence of
933 a *Wolbachia* infection frequency cline in *Drosophila melanogaster* and the possible role
934 of reproductive dormancy. *Evolution* 70:979–997.

935 Kriesner, P., A. A. Hoffmann, S. F., Lee, M. Turelli, and A. R. Weeks. 2013. Rapid sequential
936 spread of two *Wolbachia* variants in *Drosophila simulans*. *PLoS Pathogens* 9:e1003607.

937 Lachaise, D., J. R. David, F. Lemeunier, L. Tsacas and M. Ashburner. 1986. The reproductive
938 relationships of *Drosophila sechellia* with *D. mauritiana*, *D. simulans*, and *D.*
939 *melanogaster* from the Afrotropical region. *Evolution* 40:262–271.

940 Laven, H. 1951. Crossing Experiments with *Culex* Strains. *Evolution* 5:370-375.

941 Legrand, D., T. Chenel, C. Campagne, D. Lachaise and M. L. Cariou. 2011. Inter-island
942 divergence within *Drosophila mauritiana*, a species of the *D. simulans* complex: Past
943 history and/or speciation in progress? *Molecular Ecology* 20:2787–2804.

944 LePage, D. P., J. A. Metcalf, S. R. Bordenstein, J. On, J. I. Perlmutter, J. D. Shropshire, E. M.
945 Layton, L. J. Funkhouser-Jones, J. F. Beckmann, S. R. Bordenstein. 2017. Prophage WO
946 genes recapitulate and enhance *Wolbachia*-induced cytoplasmic incompatibility. *Nature*
947 543:243–247.

948 Li, H., and R. Durbin. 2009. Fast and accurate short read alignment with Burrows-Wheeler
949 transform. *Bioinformatics* 25:1754–1760.

950 Lindsey, A. R. I., D. W. Rice, S. R. Bordenstein, A. W. Brooks, S. R. Bordenstein, A. W.
951 Brooks, S. R. Bordenstein, I. L. Newton. 2018. Evolutionary Genetics of Cytoplasmic
952 Incompatibility Genes *cifA* and *cifB* in Prophage WO of *Wolbachia*. *Genome Biology*
953 and Evolution 10:434–451.

954 Lindsey, A. R. I., J. H. Werren, S. Richards and R. Stouthamer. 2016. Comparative Genomics of
955 a Parthenogenesis-Inducing *Wolbachia* Symbiont. *Genes|Genomes|Genetics*. 6:2113–
956 2123.

957 Martinez, J., B. Longdon, S. Bauer, Y.-S. Chan, W. J. Miller, K. Bourtzia, L. Teixeira, F. M.
958 Jiggins. 2014. Symbionts commonly provide broad spectrum resistance to viruses in
959 insects: A comparative analysis of *Wolbachia* strains. *PLoS Pathogens* 10:e1004369.

960 Matute, D. R., and J. F. Ayroles. 2014. Hybridization occurs between *Drosophila simulans* and
961 *D. sechellia* in the Seychelles archipelago. *Journal of Evolutionary Biology* 27:1057–
962 1068.

963 Mavingui, P., C. Valiente Moro, V. Tran-Van, F. Wisniewski-Dye, V. Raquin, G. Minard, F. H.
964 Tran, D. Voronin, Z. Rouy, P. Bustos, L. Lozano, V. Barbe, V. Gonzalez. 2012. Whole-
965 genome sequence of *Wolbachia* strain wAlbB, an endosymbiont of tiger mosquito vector
966 *Aedes albopictus*. *Journal of Bacteriology* 194:1840.

967 McDermott, S. R., and R. M. Kliman. 2008. Estimation of isolation times of the island species in
968 the *Drosophila simulans* complex from multilocus DNA sequence data. *PLoS One*
969 3:e2442.

970 Merçot, H., and D. Poinot. 1998. ...and discovered on Mount Kilimanjaro. *Nature* 391:853.

971 Merçot, H., and D. Poinot. 2003. *Wolbachia* transmission in a naturally bi-infected *Drosophila*
972 *simulans* strain from New-Caledonia. *Entomologia Experimentalis et Applicata* 86:97–
973 103.

974 Merçot, H., B. Llorente, M. Jacques, A. Atlan and C. Montchamp-Moreau. 1995. Variability
975 within the Seychelles cytoplasmic incompatibility system in *Drosophila simulans*.
976 *Genetics* 141:1015–1023.

977 Nunes, M. D., P. O. Wengel, M. Kreissl and C. Schlotterer. 2010. Multiple hybridization events
978 between *Drosophila simulans* and *Drosophila mauritiana* are supported by mtDNA
979 introgression. *Molecular Ecology* 19:4695–4707.

980 Ochman, H., and A. C. Wilson. 1987. Evolution in bacteria: evidence for a universal substitution
981 rate in cellular organisms. *Journal of Molecular Evolution* 26:74–86.

982 O'Neill, S. L., R. Giordano, A. M. Colbert, T. L. Karr and H. M. Robertson. 1992. 16S rRNA
983 phylogenetic analysis of the bacterial endosymbionts associated with cytoplasmic
984 incompatibility in insects. *Proceedings of the National Academy of Sciences* 89:2699–
985 2702.

- 986 O'Neill, S. L., and T. L. Karr. 1990. Bidirectional incompatibility between conspecific
987 populations of *Drosophila simulans*. *Nature* 348:178–180.
- 988 Pinto, S. B., K. Stainton, S. Harris, Z. Kambris, E. R. Sutton, M. B. Bonsall, J. Parkhill, S. P.
989 Sinkins. 2013. Transcriptional regulation of *Culex pipiens* mosquitoes by *Wolbachia*
990 influences cytoplasmic incompatibility. *PLoS Pathogens* 9:e1003647.
- 991 Poinot, D., K. Bourtzis, G. Markakis, C. Savakis, and H. Merçot. 1998. *Wolbachia* transfer from
992 *Drosophila melanogaster* into *D. simulans*: host effect and cytoplasmic incompatibility
993 relationships. *Genetics* 150:227–237.
- 994 Prout, T. 1994. Some evolutionary possibilities for a microbe that causes incompatibility in its
995 host. *Evolution* 48:909–911.
- 996 Raychoudhury, R., L. Baldo, D. C. S. G. Oliveira, and J. H. Werren. 2009. Modes of acquisition
997 of *Wolbachia*: horizontal transfer, hybrid introgression, and codivergence in the *Nasonia*
998 species complex. *Evolution* 63:165–183.
- 999 Reynolds, K. T., and A. A. Hoffmann. 2002. Male age, host effects and the weak expression or
1000 non-expression of cytoplasmic incompatibility in *Drosophila* strains infected by
1001 maternally transmitted *Wolbachia*. *Genetics Research* 80:79–87.
- 1002 Richardson, M. F., L. A. Weinert, J. J. Welch, R. S. Linheiro, M. M. Magwire, F. M. Jiggins, C.
1003 M. Bergman. 2012. Population genomics of the *Wolbachia* endosymbiont in *Drosophila*
1004 *melanogaster*. *PLoS Genetics* 8:e1003129.
- 1005 Ritchie S. A. 2018. *Wolbachia* and the near cessation of dengue outbreaks in Northern Australia
1006 despite continued dengue importations via travellers. *Journal of Travel*
1007 *Medicine*. 25:tay084.)
- 1008 Rousset, F., and M. Solignac. 1995. Evolution of single and double *Wolbachia* symbioses during
1009 speciation in the *Drosophila simulans* complex. *Proceedings of the National Academy of*
1010 *Sciences* 92:6389–6393.
- 1011 Satta, Y. and N. Takahata. 1990. Evolution of *Drosophila* mitochondrial DNA and the history of
1012 the *melanogaster* subgroup. *Proceedings of the National Academy of Sciences of the*
1013 *United States of America* 87:9558–9562.
- 1014 Schmidt, T. L., N. H. Barton, G. Rašić, A. P. Turley, B. L. Montgomery, I. Iturbe-Ormaetxe, P.
1015 E. Cook, P. A. Ryan, S. A. Ritchie, A. A. Hoffmann, S. L. O'Neill, and M. Turelli. 2017.
1016 Local introduction and heterogeneous spatial spread of dengue-suppressing *Wolbachia*
1017 through an urban population of *Aedes aegypti*. *PLoS Biology* 15:e2001894.
- 1018 Schrider, D. R., J. Ayroles, D. R. Matute and A. D. Kern. 2018. Supervised machine learning
1019 reveals introgressed loci in the genomes of *Drosophila simulans* and *D. sechellia*. *PLoS*
1020 *Genetics* 14:e1007341.
- 1021 Schuler, H., K. Köppler, S. Daxböck-Horvath, B. Rasool, S. Krumböck, D. Schwarz, T. S.
1022 Hoffmeister, B. C. Schlick-Steiner, F. M. Steiner, A. Telschow, C. Stauffer, W.
1023 Arthofer, M. Riegler. 2016. The hitchhiker's guide to Europe: the infection dynamics of
1024 an ongoing *Wolbachia* invasion and mitochondrial selective sweep in *Rhagoletis cerasi*.
1025 *Molecular Ecology* 25:1595–1609.
- 1026 Seemann, T. 2014. Prokka: rapid prokaryotic genome annotation. *Bioinformatics* 30:2068-2069.
- 1027 Shi, M., V. L. White, T. Schlub, J.-S. Eden, A. A. Hoffmann, E. C. Holmes. 2018. No detectable
1028 effect of *Wolbachia* wMel on the prevalence and abundance of the RNA virome of
1029 *Drosophila melanogaster*. *Proceedings of the Royal Society B: Biological Sciences*
1030 285:20181165.

1031 Shropshire, J. D., J. On, E. M. Layton, H. Zhou and S. R. Bordenstein. 2018. One prophage WO
1032 gene rescues cytoplasmic incompatibility in *Drosophila melanogaster*. Proceedings of the
1033 National Academy of Sciences. 115:4987–4991.

1034 Simao, F. A., R. M. Waterhouse, P. Ioannidis, E. V. Kriventseva and E. M. Zdobnov. 2015.
1035 BUSCO: assessing genome assembly and annotation completeness with single-copy
1036 orthologs. Bioinformatics 31:3210–3212.

1037 Siozios, S., A. Cestaro, R. Kaur, I. Pertot, O. Rota-Stabelli, and G. Anfora. 2013. Draft genome
1038 sequence of the *Wolbachia* endosymbiont of *Drosophila suzukii*. Genome
1039 Announcements. 1, e00032-13.

1040 Solignac, M. and M. Monnerot. 1986. Race formation, speciation, and introgression within
1041 *Drosophila simulans*, *D. mauritiana*, and *D. schellia* inferred from mitochondrial DNA
1042 analysis. Evolution 40:531–539.

1043 Sutton, E. R., S. R. Harris, J. Parkhill and S. P. Sinkins. 2014. Comparative genome analysis of
1044 *Wolbachia* strain wAu. BMC Genomics 15:928.

1045 Taylor, M. J., D. Voronin, K. L. Johnston and L. Ford. 2013. *Wolbachia* filarial interactions. Cell
1046 Microbiology 15: 520–526.

1047 Team, R. C. 2015. R: A language and environment for statistical computing, *R Foundation for*
1048 *Statistical Computing*, Vienna, Austria.

1049 Teixeira, L., A. Ferreira and M. Ashburner. 2008. The bacterial symbiont *Wolbachia* induces
1050 resistance to RNA viral infections in *Drosophila melanogaster*. PLoS Biology
1051 6:e1000002.

1052 Toomey, M. E., K. Panaram, E. M. Fast, C. Beatty and H. M. Frydman. 2013. Evolutionarily
1053 conserved *Wolbachia*-encoded factors control pattern of stem-cell niche tropism in
1054 *Drosophila* ovaries and favor infection. Proceedings of the National Academy of
1055 Sciences 110:10788–10793.

1056 Turelli, M. 1994. Evolution of incompatibility-inducing microbes and their hosts. Evolution
1057 48:1500–1513.

1058 Turelli, M. and N. H. Barton. 2017. Deploying dengue-suppressing *Wolbachia*: robust models
1059 predict slow but effective spatial spread in *Aedes aegypti*. Theoretical Population Biology
1060 115:45–60.

1061 Turelli, M. and A. A. Hoffmann. 1995. Cytoplasmic incompatibility in *Drosophila simulans*:
1062 dynamics and parameter estimates from natural populations. Genetics 140:1319–1338.

1063 Turelli, M., A. A. Hoffmann, and S. W. McKechnie. 1992. Dynamics of cytoplasmic
1064 incompatibility and mtDNA variation in natural *Drosophila simulans* populations.
1065 Genetics 132:713–723.

1066 Turelli, M., B. S. Cooper, K. M. Richardson, P. S. Ginsberg, B. Peckenpaugh, C. X. Antelope, K.
1067 J. Kim, M. R. May, A. Abrieux, D. A. Wilson, M. J. Bronski, B. R. Moore, J. J. Gao, M.
1068 B. Eisen, J. C. Chiu, W. R. Conner, A. A. Hoffmann. 2018. Rapid Global Spread of wRi-
1069 like *Wolbachia* across Multiple *Drosophila*. Current Biology 28:963–971.

1070 Vanthournout, B. and F. Hendrickx. 2016. Hidden suppression of sex ratio distortion suggests
1071 Red queen dynamics between *Wolbachia* and its dwarf spider host. Journal of
1072 Evolutionary Biology 29:1488-1494.

1073 Webster, C. L., F. M. Waldron, S. Robertson, D. Crowson, G. Ferrari, J. F. Quintana, J.-M.
1074 Brouqui, E. H. Bayne, B. Longdon, A. H. Buck, B. P. Lazzaro, J. Akorli, P. R. Haddrill,
1075 and D. J. Obbard. 2015. The Discovery, Distribution, and Evolution of Viruses
1076 Associated with *Drosophila melanogaster*. PLoS Biology 13:e1002210.

1077 Weeks, A. R., M. Turelli, W. R. Harcombe, K. T. Reynolds, and A. A. Hoffmann. 2007. From
1078 parasite to mutualist: rapid evolution of *Wolbachia* in natural populations of *Drosophila*.
1079 PLoS Biology 5:e114.

1080 Weinert, L. A., E. V. Araujo-Jnr, M. Z. Ahmed and J. J. Welch. 2015. The incidence of bacterial
1081 endosymbionts in terrestrial arthropods. Proceedings of the Royal Society of London B:
1082 Biological Sciences 282:20150249.

1083 Werren, J. H., and D. M. Windsor. 2000. *Wolbachia* infection frequencies in insects: evidence of
1084 a global equilibrium? Proceedings of the Royal Society B: Biological Sciences
1085 267:1277–1285.

1086 Werren, J. H., W. Zhang and L. R. Guo. 1995. Evolution and phylogeny of *Wolbachia*:
1087 reproductive parasites of arthropods. Proceedings of the Royal Society B-Biological
1088 Sciences 261:55–63.

1089 Wu, M., L. V. Sun, J. Vamathevan, M. Riegler, R. Deboy, J. C. Brownlie, E. A. McGraw, W.
1090 Martin, C. Esser, N. Ahmadinejad. 2004. Phylogenomics of the reproductive parasite
1091 *Wolbachia pipientis* wMel: a streamlined genome overrun by mobile genetic elements.
1092 PLoS Biology 2:e69.

1093 Yen, J. H. and A. R. Barr. 1971. New hypothesis of the cause of cytoplasmic incompatibility in
1094 *Culex pipiens* L. Nature 232:657-658.

1095 Zabalou, S., A. Apostolaki, S. Pattas, Z. Veneti, C. Paraskevopoulos, I. Livadaras, G. Markakis,
1096 T. Brissac, H. Merçot, K. Bourtzis. 2008. Multiple rescue factors within a *Wolbachia*
1097 strain. Genetics 178:2145–2160.

1098 Zug, R., and P. Hammerstein. 2012. Still a host of hosts for *Wolbachia*: Analysis of recent data
1099 suggests that 40% of terrestrial arthropod species are infected. PLoS ONE 7:e38544.
1100
1101
1102
1103
1104
1105
1106
1107
1108
1109
1110
1111
1112
1113
1114

1115 **Appendix 1. Mathematical analyses of mtDNA and *Wolbachia* dynamics**

1116 Our analysis follows the framework developed in Turelli et al. (1992), but is simplified by the
 1117 lack of CI. We suppose that introgression introduces a cytoplasm carrying *Wolbachia* and a
 1118 novel mtDNA haplotype, denoted B. Before *Wolbachia* introduction, we assume the population
 1119 is monomorphic for mtDNA haplotype A. With imperfect maternal *Wolbachia* transmission,
 1120 uninfected individuals will be produced with mtDNA haplotype B. Without horizontal or
 1121 paternal transmission (which are very rare, Turelli et al. 2018), all *Wolbachia*-infected
 1122 individuals will carry mtDNA haplotype B. Once *Wolbachia* is introduced, uninfected
 1123 individuals can have mtDNA haplotype A or B. We assume that these three cytoplasmic types
 1124 (“cytotypes”) differ only in fecundity, and denote their respective fecundities F_I , F_A and F_B .
 1125 Denote the frequencies of the three cytotypes among adults in generation t by $p_{I,t}$, $p_{A,t}$ and $p_{B,t}$,
 1126 with $p_{I,t} + p_{A,t} + p_{B,t} = 1$. Without CI, the frequency dynamics are

1127
 1128
$$p_{I,t+1} = \frac{p_{I,t}F_I(1-\mu)}{\bar{F}}, \quad p_{A,t+1} = \frac{p_{A,t}F_A}{\bar{F}}, \quad \text{and} \quad p_{B,t+1} = \frac{p_{B,t}F_B + p_{I,t}\mu F_I}{\bar{F}}, \quad \text{with} \quad (\text{A1})$$

1129
 1130
$$\bar{F} = F_I p_{I,t} + F_A p_{A,t} + F_B p_{B,t}. \quad (\text{A2})$$

1131
 1132 If the uninfected population is initially monomorphic for mtDNA haplotype A, the *Wolbachia*
 1133 infection frequency will increase when rare if and only if

1134
 1135
$$F_I(1-\mu) > F_A. \quad (\text{A3})$$

1136
 1137 Turelli et al. (1992) showed that if a CI-causing *Wolbachia* is introduced with a cytoplasm
 1138 that contains a novel mtDNA haplotype B, which has no effect on fitness, *Wolbachia*-uninfected
 1139 individuals will eventually all carry haplotype B. This follows because eventually all uninfected
 1140 individuals have *Wolbachia*-infected maternal ancestors. This remains true for non-CI-causing
 1141 *Wolbachia* that satisfy (A3). However, we conjectured that if the introduced B mtDNA is
 1142 deleterious in the new host nuclear background, i.e., $F_A > F_B$, a stable polymorphism might be
 1143 maintained for the alternative mtDNA haplotypes. The motivation was that imperfect maternal
 1144 transmission seemed analogous to migration introducing a deleterious allele into an “island” of
 1145 uninfected individuals. To refute this conjecture, consider the equilibria of (A1) with

1146

$$1147 \quad F_I > F_A \geq F_B. \quad (A4)$$

1148

1149 If all three cytotypes are to be stably maintained, we expect each to increase in frequency when
 1150 rare. In particular, we expect the fitness-enhancing mtDNA haplotype A to increase when the
 1151 population contains only infected individuals and uninfected individuals carrying the deleterious
 1152 *Wolbachia*-associated mtDNA haplotype B. From (A1), $p_{A,t}$ increases when rare if and only if

1153

$$1154 \quad F_A > \bar{F} = F_I p_{I,t} + F_B(1 - p_{I,t}). \quad (A5)$$

1155

1156 In the absence of haplotype A, we expect p_I to be at equilibrium between selection and imperfect
 1157 maternal transmission, i.e.,

1158

$$1159 \quad p_I = 1 - \frac{\mu F}{F - 1}, \quad (A6)$$

1160

1161 with $F = F_I/F_B$ (Hoffmann and Turelli 1997). Substituting (A6) into (A5) and simplifying, the
 1162 condition for $p_{A,t}$ to increase when rare is

1163

$$1164 \quad F_A(F_I - F_B) > F_I(1 - \mu)(F_I - F_B). \quad (A7)$$

1165

1166 By assumption (A4), $F_I > F_B$; hence (A7) contradicts condition (A3), required for initial
 1167 *Wolbachia* invasion. Thus, simple selection on *Wolbachia*-uninfected mtDNA haplotypes cannot
 1168 stably maintain an mtDNA polymorphism. The “ancestral” mtDNA haplotype A is expected to
 1169 be replaced by the less-fit *Wolbachia*-associated haplotype B.

1170 To understand the time scale over which this replacement occurs, let r_t denote the frequency
 1171 of haplotype A among *Wolbachia*-uninfected individuals, i.e., $r_t = p_{A,t}/(p_{A,t} + p_{B,t})$. From (A1),

1172

$$1173 \quad r_{t+1} = \frac{r_t F_A}{r_t F_A + (1 - r_t) F_B + \mu F_I [p_{I,t}/(1 - p_{I,t})]}. \quad (A8)$$

1174

1175 If we assume that the mtDNA haplotypes do not affect fitness, i.e., $F_A = F_B$, and that the
1176 *Wolbachia* infection frequency has reached the equilibrium described by (A6), (A8) reduces to

1177

$$1178 \quad r_{t+1} = r_t/[F(1 - \mu)], \quad (A9)$$

1179

1180 with $F = F_I/F_B$.

1181

1182

1183

1184

1185

1186

1187

1188

1189

1190

1191

1192

1193

1194

1195

1196

1197

1198

1199

1200

1201

1202

1203

1204

1205

1206 **SUPPLEMENTAL INFORMATION**

1207

1208 **Supplemental Tables**

1209

Supplemental Table 1. *w*Mau assembly statistics.

Genotype	Scaffold count	N50 (bp)	Longest scaffold (bp)	Total length (bp)
<i>R9</i>	36	60,027	169,305	1,266,004
<i>R29</i>	36	61,106	169,295	1,277,467
<i>R31</i>	39	63,676	169,381	1,272,847
<i>R41</i>	42	61,106	170,537	1,303,156
<i>R60</i>	38	63,156	221,751	1,282,564

1210

1211

1212

Supplemental Table 2. Near-universal, single-copy proteobacteria genes (out of 221) found using BUSCO v. 3.0.0.

Genome	Complete	Duplicated	Fragment	Absent
<i>w</i> Ri	179	1	2	39
<i>w</i> Mel	179	1	2	39
<i>w</i> Au	180	1	2	38
<i>w</i> Ha	178	1	3	39
<i>w</i> No	180	1	4	36
<i>R9</i>	180	1	4	36
<i>R29</i>	180	1	4	36
<i>R31</i>	180	1	4	36
<i>R41</i>	180	1	4	36
<i>R60</i>	180	1	4	36

1213

Supplemental Table 3. Copy number variants in *wMau* relative to sister *wNo*. Genomic positions are based on the *wNo* reference. There were no CNVs among *wMau* variants.

Start	End	Change	Wilcoxon Rank Sum Test	Kolmogorov-Smirnov Test
115,000	142,000	1 → 0	< 0.0001	< 0.0001
590,000	593,000	1 → 0	0.0027	0.0050
982,000	991,000	1 → 0	< 0.0001	< 0.0001
1,195,000	1,199,000	1 → 0	0.0005	0.0007

1214
1215
1216

Supplemental Table 4: Genes present in regions deleted in *wMau* relative to *wNo*. Genes predicted to be pseudogenized in *wNo* are shaded grey.

Accession number	Name
Deletion 1 (115,000-142,000):	
wNO_RS00550	Hypothetical protein
wNO_RS06015	Ankyrin repeat domain protein
wNO_RS00560	Pseudo IS256 family transposase, frameshifted
wNO_RS00565	Recombinase family protein
wNO_RS00570	DUF2924 domain-containing protein
wNO_RS00575	Ankyrin repeat domain-containing protein
wNO_RS00580	Ankyrin repeat domain-containing protein
wNO_RS00585	Phage tail protein
wNO_RS00590	Baseplate assembly protein GpJ
wNO_RS00595	Pseudo baseplate assembly protein W, frameshifted
wNO_RS00600	Hypothetical protein
wNO_RS00605	Phage baseplate assembly protein V
wNO_RS00610	Hypothetical protein
wNO_RS00615	Putative minor tail protein Z
wNO_RS00620	Hypothetical protein
wNO_RS00625	Minor capsid protein E
wNO_RS00630	Head decoration protein
wNO_RS00635	S49 family peptidase

wNO_RS00640	Pseudo phage portal protein, frameshifted
wNO_RS00645	Phage head stabilizing protein GpW
wNO_RS00650	Phage terminase large subunit family protein
wNO_RS00655	Ankyrin repeat domain-containing protein
wNO_RS00660	Hypothetical protein
wNO_RS00665	Hypothetical protein
wNO_RS00670	Sigma-70 family RNA polymerase sigma factor
wNO_RS00675	ATP-binding protein
wNO_RS00680	IS110 family transposase
Deletion 2 (590,000-593,000):	
wNO_RS02645	XRE family transcriptional regulator
wNO_RS02650	Hypothetical protein
wNO_RS02655	Hypothetical protein
wNO_RS02660	XRE family transcriptional regulator
Deletion 3 (982,000-991,000):	
wNO_RS04690	Group II intron reverse transcriptase/maturase
wNO_RS06355	Hypothetical protein
wNO_RS04695	Pseudo hypothetical protein, partial
wNO_RS04700	Pseudo cell filamentation protein Fic, partial
wNO_RS04705	Hypothetical protein
wNO_RS04710	DNA methylase
wNO_RS04715	Hypothetical protein
wNO_RS04720	Ankyrin repeat domain-containing protein
wNO_RS04725	Phage terminase large subunit family protein
wNO_RS04730	Phage head stabilizing protein GpW
wNO_RS04735	DUF1016 domain-containing protein
Deletion 4 (1,195,000-1,199,000):	
wNO_RS06095	Ankyrin repeat domain protein
wNO_RS05590	Rpn family recombination-promoting nuclease/putative transposase

1217
1218

Supplemental Table 5. *w*Mau does not significantly affect *D. mauritiana* fecundity in comparisons of paired infected (I) and uninfected (U) strains sharing host nuclear backgrounds. *N* is the number of females that produced the means and SDs. *P* values are for two-tailed Wilcoxon tests. Cytoplasm sources are denoted with superscripts for introgressed strains.

Strain	Mean eggs laid/5 days	SD	<i>N</i>	<i>P</i> value
<i>R3II</i>	210.97	55.22	30	0.901
<i>R3IU</i>	213.50	58.43	28	
<i>R4II</i>	265.43	31.47	30	0.355
<i>R4IU</i>	239.69	73.43	29	
<i>R3I^{R4I}I</i>	257.83	58.15	30	0.762
<i>R3I^{R4I}U</i>	254.67	48.72	30	
<i>R4I^{R3I}I</i>	248.77	45.54	30	0.433
<i>R4I^{R3I}U</i>	250.67	76.35	30	

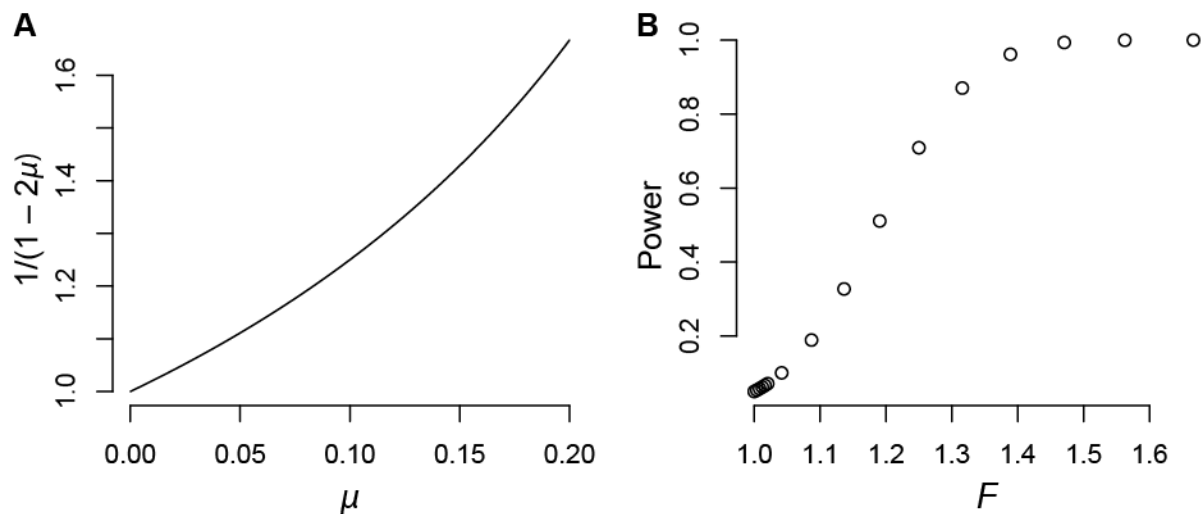
1219

1220

1221

1222 **Supplemental Figures**

1223



1224

1225

1226

1227

1228

Supplemental Figure 1. A) Our proposed upper bound, $1/(1 - 2\mu)$, on plausible relative fitness, F , as a function of μ ranging from perfect transmission ($\mu = 0$) to a level of imperfect transmission ($\mu = 0.2$) that has not been observed in nature. B) Our power to detect values of F .